Function of STAT5A in Osteogenic Differentiation and Bone Formation

Kyoung Mi Lee

Department of Medical Science
The Graduate School, Yonsei University

Function of STAT5A in Osteogenic Differentiation and Bone Formation

Directed by Professor Jin Woo Lee

The Doctoral Dissertation submitted to the Department of Medical Science, the Graduate School of Yonsei University in partial fulfilment of the requirements forthe degree of Doctor of Philosophy

Kyoung Mi Lee

December 2015

This certifies that the Doctoral Dissertation of Kyoung Mi Lee is approved.

Thesis Supervisor: Jin Woo Lee

Thesis Committee Member#1: Sahng Wook Park

Thesis Committee Member#2: Yumie Rhee

Thesis Committee Member#3: Jeon Han Park

Thesis Committee Member#4: Jae Myun Lee

The Graduate School
Yonsei University

December 2015

TABLE OF CONTENTS

LIST OF FIGURES

LIST OF TABLES

Abstract

Function of STAT5A
in Osteogenic Differentiation and Bone Formation

Kyoung Mi Lee

Department of Medical Science
The Graduate School, Yonsei University

(Directed by Professor Jin Woo Lee)

The regulation of osteogenesis in human bone marrow-derived stromal cells (hBMSCs) is important for bone formation. Despite advances in understanding the molecular mechanism of osteogenesis, crucial modulators in a fracture healing are not well investigated. Signal transducer and activator of transcription 5 (STAT5A) is vital for proliferation, differentiation, and survival of various cells. To investigate the role of STAT5A in osteogenesis, I performed knockdown of *Stat5a* using small interfering RNA and STAT5 inhibitor. The suppression of STAT5A increased the osteogenic differentiation and distal-less homeobox 5 (DLX5) protein expression, whereas the inhibition of STAT5B only partially increased differentiation. Subsequent gene expression profiling and RT-qPCR analyses of STAT5A inhibition led to transcriptional activity of DLX5, osteogenic transcription factor, in osteogenesis of hBMSCs. Chromatin immune-precipitation (ChIP) assays analyzing the

corresponding gene loci identified STAT5A binding sites on the promoter region of DLX5. I propose that STAT5A control osteogenesis throughout regulating transcription level of DLX5. To better characterize the contribution of STAT5A in bone formation, I generated mice with deletion of *Stat5a* (*Stat5a* $^{-/-}$ mice) and analyzed their bone phenotype. *Stat5*$^{-/-}$ mice exhibited increased bone-formation compared to wild type mice. And, the expression level of DLX5 protein was increased in mBMSCs of *Stat5*$^{-/-}$ compared to wild type mice. To evaluate the role of osteoblast activity of *Stat5*$^{-/-}$ mice in bone repair, femoral fracture healing was compared with wild-type control mice. With respect to fracture healing, total callus of *Stat5*$^{-/-}$ mice was larger than wild-type mice fractures at post fracture 2 weeks. Surprisingly, soft callus of *Stat5*$^{-/-}$ mice was organized rapidly to hard bone at post fracture 4 weeks. In summary, I show that the suppression of STAT5A activates distal-less homeobox 5 (DLX5) and enhances osteogenesis in vitro and in vivo. *Stat5a* knockout (*Stat5a* $^{-/-}$) mice are protected from age-related osteoporosis, caused by loss of bone density and strength. In a murine model of fracture repair, lack of *Stat5a* leads to significant enhancement in a bone healing process by stimulating the formation of new bones. Cartilaginous callus of *Stat5a* $^{-/-}$ mice organized to bony callus faster than that of wild type mice. Taken together, these findings suggest that STAT5A plays a role in osteogenesis and bone formation via modulation of DLX5.

Key words: osteogenesis, STAT5A, DLX5, bone formation, transcriptional activity, femoral fracture healing

Function of STAT5A
in Osteogenic Differentiation and Bone Formation

Kyoung Mi Lee

Department of Medical Science
The Graduate School, Yonsei University

(Directed by Professor Jin Woo Lee)

Ⅰ. INTRODUCTION

Human bone-marrow mesenchymal stromal cells (hBMSCs) can differentiate to osteoblast, chondrocyte, adipocyte, and tenocyte by the culture conditions. Especially, osteoblast differentiation is important to increase bone mass. Also, the proper balance between osteogenesis and adiopogenesis, which are tightly regulated by proteins, hormones, and other genes[1-5], is crucial to maintain bone homeostasis. However, if the regulation is disrupted, it can lead osteoporosis[6].

The osteogenic differentiation of hBMSCs is well characterized according to the timely expressed genes such as alkaline phosphatase (ALP), runt-related transcription factor 2 (RUNX2), distal-less homeobox 5 (DLX5), osterix (OSX) and osteocalcin (OCN) followed by extracellular matrix synthesis and mineralization[7,8]. RUNX2 has been characterized as the master transcription factor of osteogenic differentiation and bone formation[9,10]. Another transcription factor, DLX5, is expressed in all bones and

differentiating osteoblasts. DLX5 is an important regulator for the development of mineralized tissues because it induces expression of RUNX2 in BMP-signaling pathway[11,12]. DLX5 also is related to osteoblast maturation[12] and *Dlx5*$^{-/-}$ mice has severe craniofacial abnormalities and show delayed ossification of dermatocranial bones[13]. It suggests that *Dlx5* gene may plays a role in bone formation and fracture healing.

The signal transducers and activators of transcription (STAT) family plays important roles in cell proliferation, differentiation, and survival by cytokine, growth factor, and hormone reaction[14,15]. Like other STAT family members, STAT5 was originally identified as a cytosolic signaling molecule involved in proliferation, differentiation and apoptosis in cancer cells[16,17]. After the stimulation of various cytokines, STAT5 is phosphorylated and dimerized[18,19]. STAT5 dimer is translocated into the nucleus and bind to interferon-γ activated sequence (GAS) motifs followed by transcription of target genes[15,20,21]. There are two isoforms of STAT5 which are STAT5A and STAT5B. Interestingly, STAT5A and STAT5B are encoded by separate genes, but the proteins are 90% identical at the amino acid levels[18]. They have distinct functions, as revealed by several *in vivo* studies[22,23]. Recently, STAT5 was found to play as negative regulator of the bone-resorbing function in osteoclasts *in vitro* and *in vivo*[24]. One study reported that STAT5-RUNX2 interaction promotes the osteoblast differentiation *in vitro*. However, there was no report to distinguish isoforms of STAT5 in osteoblast differentiation. Previously, I demonstrated that STAT5A plays a major role in adipogenesis of hBMSCs and STAT5B has only a supportive function[25], suggesting that STAT5A plays an essential role for a bone homeostasis via the balance

between osteogenesis and adipogenesis. Here I focused on the role of STAT5A in osteoblasts to clarify which STAT5 isoform contributes to the osteoblast differentiation and provide therapeutic potentials in bone diseases.

In this study, I have found that STAT5A play an important role in bone formation and regeneration. I provide evidences that inhibition of STAT5A promotes osteoblast differentiation and bone formation through the activation of DLX5 signaling. STAT5A deletion significantly decreased bone loss in a murine age-related osteoporosis model. Moreover, in a murine fracture model, I show that STAT5A deletion enhances a bone healing by stimulating the new bone formation. These findings reveal the inhibitory function of STAT5A in osteogenesis, suggesting a therapeutic potential of STAT5A inhibition in age-related osteoporosis and fracture healing.

Ⅱ. MATERIALS AND METHODS

1. Cell culture and differentiation condition

Human bone marrow derived MSCs (hBMSCs) were taken from the posterior iliac crests of 10 adult donors aged 21-51 years, after receiving approval from the Institutional Review Board (IRB). hBMSCs were selected by their natural tendency to adhere to the culture dish. The primary hBMSCs were cultured in growth medium, Dulbecco's Modified Eagle's Medium - low glucose (DMEM-LG; Gibco, Carlsbad, CA, USA) with 10% fetal bovine serum (FBS; Gibco), 1% antibiotic- antimycotic solution (Invitrogen, Grand Island, NY, USA) and the confluence was achieved within 7 days in 5% CO_2 at 37°C. For osteogenesis, cells were cultured in DMEM-LG with 1 μM dexamethasone (Sigma, St. Louis, MO, USA), 10 mM β-glycerophosphate (Sigma) and 50 μM ascorbic acid (Sigma) for 14 days. Mouse bone marrow derived MSCs (mBMSCs) have been isolated from femurs and tibias of 3-5 mice at 10-30 weeks old. mBMSCs were cultured in growth medium (*α*- Minimum Essential Medium (α-MEM, Gibco) with 10 % FBS, 1 % antibiotic antimycotic solution, and 2 mM L-glutamine (Invitrogen, Carlsbad, CA, USA) in 5% CO_2 at 37°C[26]. To induce osteogenic differentiation the cells were cultured in growth medium with 10 mM β-glycerophosphate and 50 μM ascorbic acid for 10 days. mBMSCs were induced for the adipogenic differentiation with DMEM-high glucose (DMEM-HG, Gibco) medium containing 10% FBS, 1% antibiotic antimycotic solution, 1 μM insulin (Roche Diagnostics, Rotkreuz, Switzerland), 1 mM dexamethasone, and 0.5 mM 3-

isobutyl-1-methylxanthine (IBMX, Sigma) until 2 days. Then, the cells were cultured in DMEM-HG with 10% FBS and 1 μM insulin for 2 days and every other day cultured in DMEM-HG with 10% FBS and 1% antibiotic antimycotic solution for 21 days. For osteoclastogenesis, mice bone marrow monocyte cells (mBMMs) were cultured for 3-4 days in α- MEM containing 15 ng/ml mRANKL (R&D systems, Minneapolis, MN, USA) and 40 ng/ml mMCSF (R&D systems)[27].

2. Plasmid constructs

Recombinant plasmids of pcDNA-mStat5a and pcDNA-mStat5b were kindly gifted from Dr. Hiroko Yamashita (Nagoya City University, Nagoya, Japan). pcDNA-hSTAT5A, pcDNA-hSTAT5B, and pcDNA-hDLX5 were constructed by amplifying each coding regions from cDNA of HeLa cells. And all promoter vectors were obtained with PCR of human genomic DNA. Human DLX5 and STAT5A promoter region spanning -2208/+ 142 bp and - 2121/+ 88 bp were inserted into pGL3 basic vector (Addgene, Cambridge, MA, USA) and named pGL-DLX5 Full and pGL-STAT5A, respectively. pGL-DLX5 Del1 to pGL-DLX5 Del4, containing 5' serial deletions fragments of the DLX5 promoter, were cloned by amplifying the regions from - 2003 to + 142, - 1751 to + 142, - 1254 to + 142, and - 645 to + 142 bp, respectively. **(Fig. 1)**.

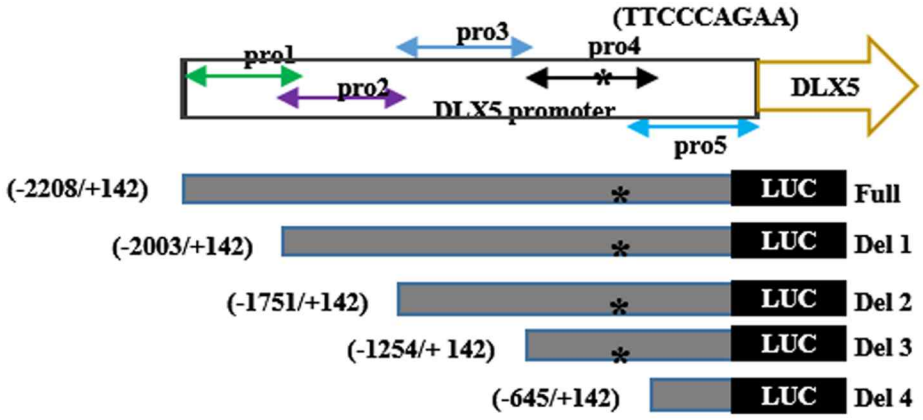

Figure 1. A schematic design for predicted STAT5A binding site on DLX5 promoter and DLX5 promoter deletion constructs. For a ChIP assay, STAT5A binding sequence (*) on DLX5 promoter region was predicted using the TESS program (upper). For the promoter activity analysis, 5' truncated - DLX5 promoter-luciferase constructs were generated (bottom).

3. Gene transfection and luciferase reporter assay

Recombinant plasmids were transfected into hBMSCs using lipofectamine LTX and plus reagent (Invitrogen) according to the manufacturer's protocol. Then, the medium was replaced with 2 ml DMEM-LG with 10% FBS and 1% antibiotic antimycotic solution or osteogenic medium. After 24 hrs, the cells were lysed with 200 μl of 1× passive lysis buffer (Promega, Madison, WI, USA) per tube, and cell debris was removed. Luciferase activity was measured by the dual-luciferase reporter assay kit (Promega). Relative luciferase activity were normalized by *renilla* activities to adjust transfection efficiency. The assays were performed at least three times.

4. Inhibition of STAT5A and STAT5B

Synthetic siRNAs for STAT5A and STAT5B mRNA were purchased from Bioneer (Daejeon, South Korea). The 80% confluence hBMSCs were transfected with each siRNA by lipofectamine LTX (Invitrogen). After 36 hrs, the cells were collected and prepared for analysis. The silencing effects of the siSTAT5A and siSTAT5B were checked by reduced protein expression of STAT5A and STAT5B. The negative control duplexes (Bioneer, Korea) were used as a negative control. A STAT5 inhibitor (sc-355979) was purchased from Santa Cruz Biotechnology (Dallas, TX, USA)

5. Isolation of mRNA and quantitative RT- PCR analysis

Total RNA was isolated by the RNeasy Mini Kit (Qiagen, Venlo, Netherlands) according to the protocol by the manufacturer. For quantitative RT-PCR, cDNA was synthesized by oligo dT_{18} primer (Invitrogen) on the isolated RNA as a template and

Omniscript Reverse-Transcription Kit (Qiagen) according to manufacturer's instructions. And, the RT- PCR was performed using 2x qPCRBIO SyGreen Mix Hi-Rox (PCR Biosystems, London, UK) and analyzed by ABI STEPONE PLUS system (ABI, Carlsbad, CA, USA). All primers were purchased from Bioneer. The relative expression of each gene was normalized by GAPDH expression. The specific primer pairs are shown in **Table 1 and 2.** All reactions have been performed in triplicate. Relative expression levels and S.D. values were evaluated by the comparative method.

Table 1. A list of primers used for RT-PCR for human osteoblast related genes in this study

Gene symbol		Sequences (5'--> 3')
STAT5A	Forward	CAGTGGTTTGACGGGGTGAT
	Reverse	GTCGTGGGCCTGTTGCTTAT
STAT5B	Forward	ACTGCTAAAGCTGTTGATGGATAC
	Reverse	TGAGTCAGGGTTCTGTGGGTA
DLX5	Forward	GAGTAGGTGTCCCGCCTCAGAACCC
	Reverse	CCAACCAGCCAGAGAAAGAA
RUNX2	Forward	TACAAACCATACCCAGTCCCTGTTT
	Reverse	AGTGCTCTAACCACAGTCCATGCA
BSP	Forward	ATAC CATCTCACACCAGTTAGAATG
	Reverse	AACAGCGTAAAAGTGTTCCTATTTC
GAPDH	Forward	CTGCTGATGCCCCCATGTTC
	Reverse	ACCTTGGCCAGGGGTGCTAA

Table 2. A list of primers used for RT-PCR for mice genes in this study

Gene symbol		Sequences (5'--> 3')
Stat5a	Forward	ATGGGGA CTATGATC CAGGC
	Reverse	CCCAGCTTGATCTTCAGCAA
Stat5b	Forward	GGACTCCGTCCTTGATACCG
	Reverse	TCCATCGTGTCTTCCAGATCG
Dlx5	Forward	GCTAGATGGGCTACTTTCTCTT
	Reverse	GCGTTCAAACATCCCCGTATGA
Alp	Forward	CACAATATCAAGGATATCGACGTGA
	Reverse	ACATCAGTTCTGTTCTTCGGGTACA
Bsp	Forward	CCGGCCACGCTACTTTCTT
	Reverse	TGGACTGGAAACCGTTTCAGA
Opn	Forward	GCCGAGGTGATAGTGTGGTT
	Reverse	TGAGGTGATGTCCTCGTCTG
Ocn	Forward	AGCAAAGGTGCAGCCTTTGT
	Reverse	CTTCACTACCTCGCTGCCCT
Pparγ	Forward	GAAACTCTGGGAGATTCTCCT
	Reverse	CAGAGCTGATTCCGAAGTTGG
Adiponectin	Forward	AGCCGCTTATATGTATCGCTCA
	Reverse	TGCCGTCATAATGATTCTGTTGG
Leptin	Forward	AAGAAGATCCCAGGGAGGAA
	Reverse	TGATGAGGGTTTTGGTGTCA
Opg	Forward	CGGAAACAGAGAAGCCACGCAA
	Reverse	CTGTCCACCAAAACACTCAGCC
Rankl	Forward	CAGCATCGCTCTGTTCCTGTA
	Reverse	CTGCGTTTTCATGGAGTCTCA
Gapdh	Forward	GTGTTCCTACCCCCAATGTGT
	Reverse	ATTGTCATACCAGGAAATGAGCTT

6. Western blot analysis and antibodies

Collected cells were washed 2 times with 1X PBS and lysed by the 100 μl of whole cell lysis buffer (60 mM Tris-HCl, pH 6.8, 1% SDS) for 10 min at 100°C. Collected supernatants, followed by centrifugation at 13,000 rpm for 10 min, were quantified using a BCA protein assay kit (Thermo Scientific, Rockford, IL, USA). For western blot analysis, a total of 25 μg protein were separated on the 10% SDS- PAGE in reducing condition. Subsequently, the proteins were transferred onto Polyvinylidene difluoride (PVDF) membrane (Amersham, Pharmacia, Piscataway, NJ, USA) in transfer buffer (1.4% glycine, 20% methanol and 25 mM Tris-HCl, pH 8.3 for 90 min at 70 V. After that, membranes were incubated in blocking solution [1X TBST (50 mM Tris-HCl, 150 mM NaCl, and 0.1 % Tween- 20) contained 5% skimmed milks] for 1 hr at room temperature. And then, blocked membranes were incubated in 1% skim milk solution including primary antibodies for overnight at 4°C. Membranes were washed 3 times with 1X TBST followed by incubation with secondary antibodies for 1 hr at room temperature. Primary antibodies used for blotting were anti-STAT5A (1: 1000, Abcam, Cambridge, UK), anti-STAT5B (1: 1000, Abcam), anti-DLX5 (1: 500, Abcam), and anti-Runx2 (1: 1000, Millipore, Molsheim, France). And all reactions were visualized by autoradiography using the ECL Plus and ECL Western Blotting detection systems (Amersham BioSciences, Buckinghamshire, UK). And signal intensities were determined by densitometry analysis using the image J program.

7. Chromatin immunoprecipitation (ChIP) analysis

ChIP analysis was performed using ChIP assay kit (Upstate Biotechnology, Charlottesville, VA, USA) and followed the protocol of kit manual. Briefly, hBMSCs were induced to osteoblast for 3 days and the differentiated cells were cross-linked with 1% formaldehyde solution for 10 min at room temperature. The cross-linked cells were lysed with SDS lysis buffer and sonicated. The DNA-protein complexes were bound with antibody against STAT5A (Abcam, 1:1000) and the immune complexes were collected by binding with a protein A-agarose for overnight at 4℃. After washing the complexes with 1X PBS, DNA was extracted by phenol/chloroform alcohol precipitation and used as the DNA templates for amplifying the DNA fragments. The specific primer pairs for DLX5 promoter are shown in **Table 3.**

Table 3. Specific primer sequences for ChIP analysis

Primer name		Sequences (5'--> 3')
Pro 1	Forward	CTAGCAAGCAGTTTGCAACC
	Reverse	GGCGAATGAAGCATTCACAC
Pro 2	Forward	TACTCCATCGCTCCCAACTG
	Reverse	GGTTGCAAACTGCTTGCTAG
Pro 3	Forward	CCCTCCTTTTGTTTACTTTGG,
	Reverse	CAGTTGGGAGCGATGGAGTA
Pro 4	Forward	CATGCAGGAGGATTACCT
	Reverse	CAAATGTCCAGAACCTTTTCAG
Pro 5	Forward	AGCAATGGAGAA GCAAGATACC
	Reverse	GCAGGTAATCCTCCTGCATG

8. Alkaline phosphatase (ALP) staining and activity

The mBMSCs were fixed in a solution of citrate working solution: acetone (2:3, v/v) for 30 sec and washed in distilled water for 1 min. ALP staining was performed with a fast violet B salt kit (Sigma Aldrich). The cells were then placed in an ALP staining solution for 30 min and washed 2 times with distilled water. ALP activity of mBMSC was determined by a colorimetric assay at day 0. The cells were washed 2 times with ice-cold PBS and harvested 0.5 ml 50 mM Tris–HCl, pH 7.6. After sonication and centrifugation for 15 min at 12000 *rpm*. Alp activity of the supernatant was measured using *p*-nitrophenylphosphate released per min per μg total protein at 405nm. Total cellular protein amount was determined using a BCA assay kit.

9. Von Kossa and Alizarin red S staining

Osteogenic differentiated cells were washed 2 times with PBS and fixed in a solution of acetone: methanol (1:1, v/v) and 70% ethanol for von kossa and alizarin red S staining, respectively. And then, the cells were washed with distilled water several times and stained with 3% silver nitrate solution and 2% Alizarin red S solution for 30 min, respectively. Destaining of the alizarin red S samples were eluted by 10% (weight volume) cetylpyridinium chloride for 30 min at room temperature. And then, the supernatants were measured in a microplate reader at $A_{595\ nm.}$

10. Animals

Stat5a general knockout mice (C57BL/6 background) were obtained from Lothar Hennighausen Laboratory (Bethesda, Maryland, USA). The deletion of the *Stat5a* gene was determined by PCR around the substituted neomycin gene site using the specific primer. The primer pairs are shown in **Table 4.** The littermates of *Stat5a*$^{-/-}$ mice were generated by intercrossing *Stat5* Ht (*Stat5a*$^{+/-}$) male mice with *Stat5* Ht (*Stat5a*$^{+/-}$) female mice. All experiments were performed in Animal Care center and controlled under AAALAC International (Association for Assessment and Accreditation of Laboratory Animal Care International) in Yonsei University College of Medicine, Korea. The protocol was approved by the Committee on the Ethics of Animal Experiments of Yonsei University College of Medicine (Permit Number: 2013-0401, 2014-0033).

Table 4. The primer sequence for genotyping of *Stat5a*$^{-/-}$ mice

Gene symbol		Sequences (5'--> 3')
Stat5a	Forward	CTGGATTGACGTTTCTTACCTG
	Reverse	TGGAGTCAACTAGTCTGTCTCT
Neo	Forward	AGAGGCTATTCGGCTATGACTG
	Reverse	TTCGTCCAGATCATCCTGATC

11. Micro CT analysis

I have dissected femurs without soft tissue from mice and fixed them in 70 % ethanol for 24 hrs at room temperature. The fixed femurs were analyzed by high-resolution μCT (Skyscan-1076). The image reconstruction and analysis were performed using NRecon v 1.6.6.0 and CTAn v 1.13.2.1, respectively. The parameters of the trabecular bone in the epiphysis were analyzed using 3D-model visualization software CTVol v 2.0. The acquisition setting conditions were followed by X-ray source voltage 70kVp and current 140μA. And, beam hardening reduction depended on a 0.5mm thick aluminium filter. The pixel size was 18um, exposure time 14.7sec, the rotation step 0.5°, full rotation over 360°. The quantitative analysis region of bone parameters were fixed at 1.7mm part under the growth plate. The 3D bone parameters of 10 weeks mice analyzed included: TV (total tissue volume; contains both trabecular and cortical bone), BV/TV (trabecular bone volume per tissue volume), Tb. N (trabecular number), Tb. Th (trabecular thickness), Tb. Sp (trabecular separation), BMD (bone mineral density), Bone volume (cortical bone volume), Cs. Th (cortical crossectional thickness), and Cs. area (cortical crossectional area).

12. Murine fracture model

A standardized mid-diaphyseal fracture was induced in 24 wild-type mice and 24 *Stat5a*$^{-/-}$ 6 week old mice. Mice were anesthetized with the Zoretil® (30 mg per body weight) / Rompon® (10 mg per kg body weight) by intraperitoneal injection and the right hind legs were shaved and disinfected. The femoral condyles were exposed through an incision and the femur was severed in the middle with a mess. The severed

femur was fixed by an intramedullary pin with diameter of 0.8mm. Then, the surgical wound was cleaned using physiological saline and closed by suture. Immediately after fracture, I monitored the surgical condition with micro CT **(Fig. 2)**. The mice were killed at 2 and 4 weeks (n=16 and n=32 per time point, respectively) after fracture. There were no complications and animal death during the surgery and post-operative management except for slight swelling at the surgical site. Sixteen mice (8 in *Stat5a*$^{-/-}$group and 8 in wild group) at 4 weeks point were used for mechanical test and the other (32 in each group) were used for BMD measurement (at each time point), micro-CT analysis of callus formation and mineralization (at each time point). The calcified callus volume was determined by subtracting the cortical bone volume from the total volume. Before these examinations, the femurs were extracted and the intramedullary pins were removed. The protocol was approved by the Committee on the Ethics of Animal Experiments of Yonsei University College of Medicine (Permit Number: 2014-0033).

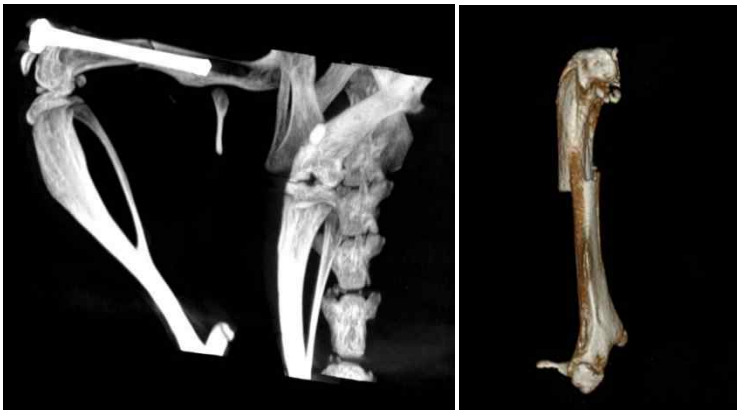

Figure 2. Micro-CT image of fractured mice femur immediately after fracture. The femoral condyles were severed in the middle with a mess and the severed femur was fixed by an intramedullary pin with diameter of 0.8 mm. The micro CT image was photographed at day 0.

13. Biomechanical testing

At eight weeks un-fractured group and 4 weeks after fracture group, femurs of 8 wild-type and *Stat5a*$^{-/-}$ mice in each group were rehydrated at room temperature in PBS and their biomechanical properties were measured using a three-point bending method. Strength tests were performed on the right femur mid-shaft using a mechanical testing machine (model 5942; Instron, Norwood, MA, USA) as condition of a displacement rate of 10 mm/min (span length, 10 mm). The maximum load [F = load (N, lb)] was determined using load- deflection diagrams.

14. Histology and immunohistochemistry

The fractured femurs were removed from 8 mice of each group and fixed in 3.7% paraformaldehyde solution for 5-7 days at room temperature and decalcified in ethylene-diamine tetraacetic acid (EDTA) glycerol solution for 1 day at room temperature. Decalcified femurs were embedded in paraffin block. The paraffin sections were dehydrated by passage through an ethanol series, cleared twice in xylene and embedded in paraffin, after which 5mm sections were cut on a rotary microtome. Decalcified femoral sections were stained with masson's trichrom, safranin O and fast green. For immune histochemistry, antigen retrieval was performed using citrate buffer, pH 6.0, for the deparaffinized sections. Sections were blocked with 5 % normal goat serum, without PBS and 0.1% Tween 20 for 1 hr at room temperature. And they were incubated with the DLX5 antibody (1: 100, EPR4488, Abcam) for 1 hr at 4°C and with anti-rabbit secondary antibodies for 1 hr at room temperature. And the DAB staining (ab64238, Abcam) was performed.

15. Statistical analysis

Data are shown as the mean ± S.D. No animals or samples were excluded from analysis. MicroCT analysis was performed in a blinded fashion. For checking normal distributions of the groups, I first performed normality test with the Shapiro-Wilk method. If normality tests passed, two-tailed, unpaired Student's *t* tests were used for the comparisons between two groups; if normality tests failed, Mann-Whitney tests were used for the comparisons between two groups. For the comparisons of three or four groups, I used one-way ANOVA if normality tests passed, followed by Tukey`s multiple comparison test for all pairs of groups. If normality tests failed, Kruskal-Wallis test was performed and followed by Dunn`s multiple comparison test. The GraphPad PRISM software (v5.0) was used for statistical analysis. $P < 0.05$ was considered statistically significant. *, $P < 0.05$; **, $P < 0.01$; ***, $P < 0.001$.

Ⅲ. RESULTS

1. Overexpression of STAT5A suppress osteogenic differentiation in hBMSCs

To investigate the possible role of STAT5 during osteogenesis, I first checked whether STAT5 expressed in hBMSCs and moved to nucleus during the osteogenesis. STAT5 was increasingly translocated into the nucleus at 1, 5, 7th day after the induction of osteogenesis **(Fig. 3a)**. To clarify STAT5 isoforms, I then examined STAT5A and STAT5B expressions during osteogenesis of hBMSCs. Intriguingly, STAT5A was increased in response to the induction of osteogenesis after 6th day **(Fig. 3b)**. The expressions of STAT5B, however, were no remarkable change during osteogenesis while DLX5 and RUNX2, which are key osteogenic marker, were decreased in the late stage of osteogenesis.

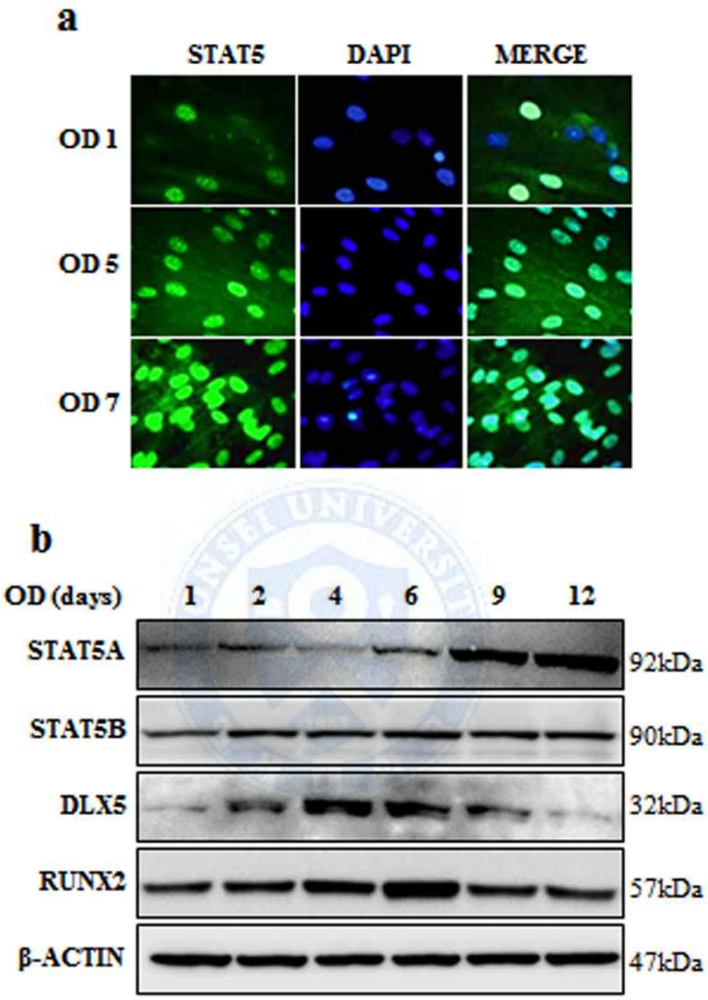

Figure 3. Expression level of STAT5 protein during osteogenesis in hBMSCs. (a) Immunocytochemistry for STAT5 translocation into nucleus at osteogenic differentiation at day 0, 5, and 7. Magnification: 100 x. **(b)** Protein level of STAT5A, STAT5B, DLX5, and RUNX2 during osteogenesis of hBMSCs by western blotting. *β*-actin was used as a control.

To examine the effect of STAT5A and STAT5B in osteogenesis, I overexpressed STAT5A and STAT5B in hBMSCs. At 14th day after the induction of osteogenesis, the mineralization of STAT5A-overexpressed hBMSCs was decreased compare to those of control hBMSCs and STAT5B-overexpressed hBMSCs **(Fig. 4a and 4b)**. Following alizarin red S staining and quantification, I also confirmed protein levels of osteogenic marker genes such as DLX5 and RUNX2. Overexpression of STAT5A in hBMSCs significantly decreased DLX5 expression, not RUNX2 expression. Overexpression of STAT5B, however, had no effect on those proteins **(Fig. 4c and 4d)**. Accordingly, STAT5A decreased mRNA levels of DLX5 and its downstream genes such as bone sialoprotein (BSP) and osteopontin (OPN) **(Fig. 5)**. These findings imply that STAT5A functions during osteogenesis of hBMSCs by regulating DLX5.

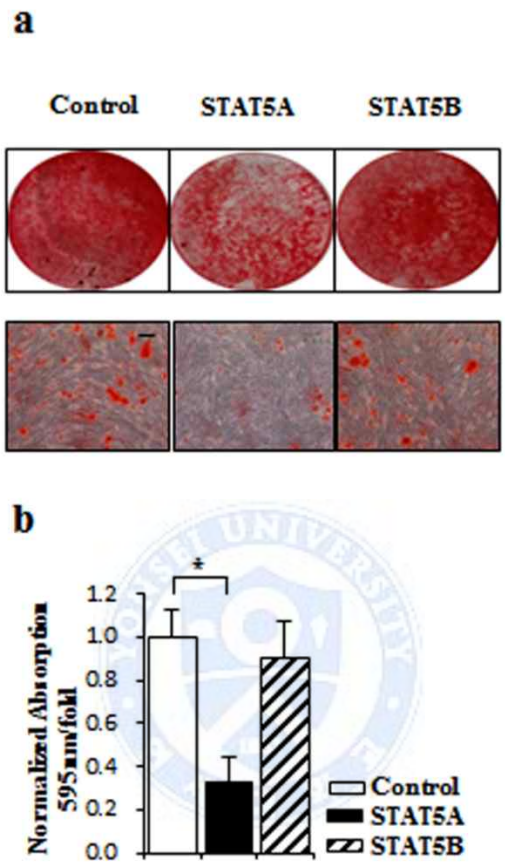

Figure 4. Suppressed osteoblastic differentiation of hBMSCs by overexpression of STAT5A. (a) Alizarin red S staining for effect of STAT5 overexpression at osteogenesis 14 days. Scale bar, 60 μm. **(b)** Quantification of alizarin red S staining.

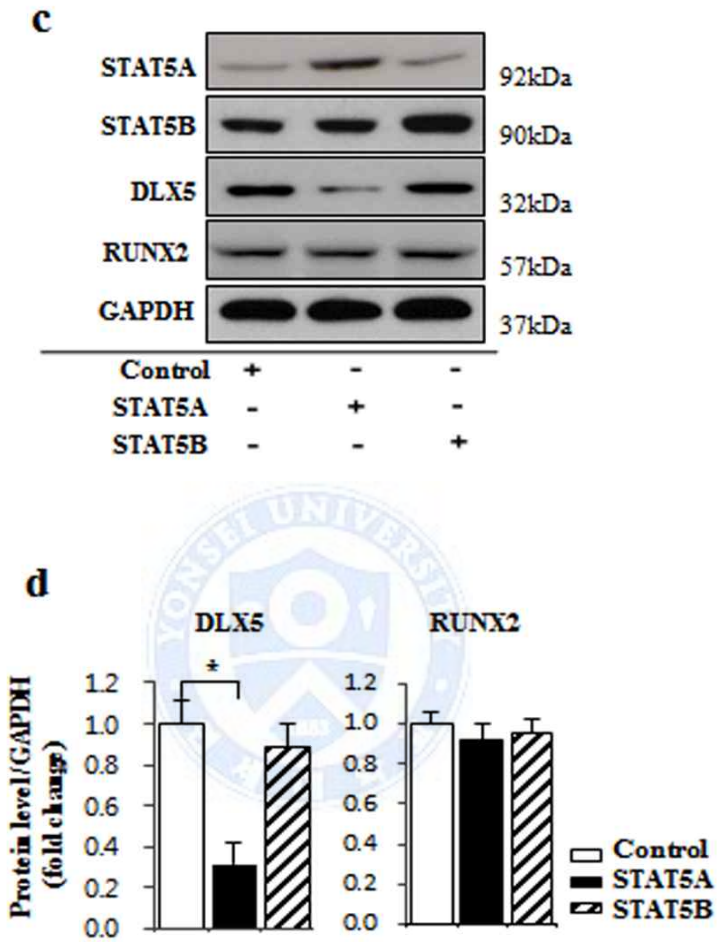

Figure 4. Suppressed osteoblastic differentiation of hBMSCs by overexpression of STAT5A. (c) Western blot analysis for protein expression level of osteogenic master proteins such as DLX5 and Runx2 by STAT5 overexpression. GAPDH was used as a control. **(d)** Quantification of DLX5 and RUNX2 protein levels.

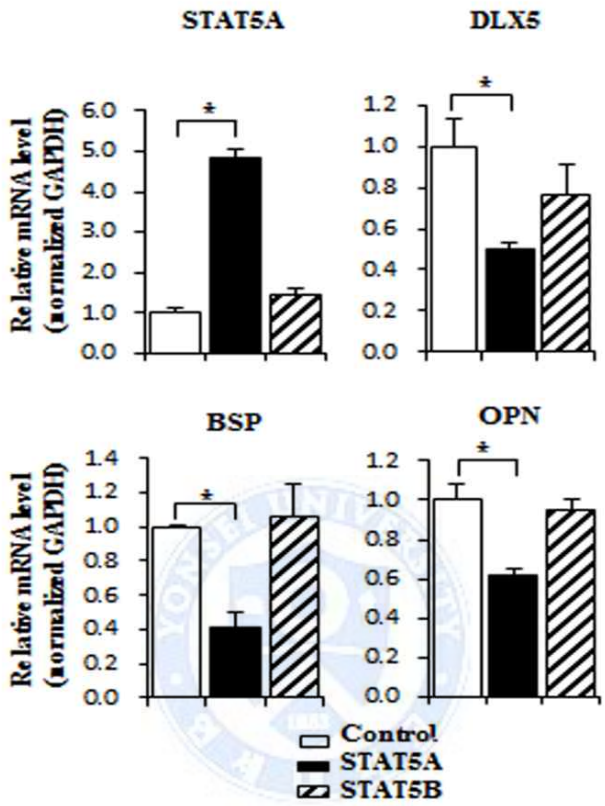

Figure 5. Suppressed mRNA expression of the osteoblast related genes by overexpression of STAT5A. Gene expression of DLX5 and downstream genes of DLX5 after 4 days of STAT5 overexpression in hBMSCs using real-time PCR. All mRNA levels were normalized with GAPDH. All experiments were performed in triplicate. All data are the mean ± S.D. (**P* < 0.05), compared to pcDNA transfected cells. Statistical significance was determined by Student's t- test.

2. Suppression of STAT5A promotes osteogenic differentiation in hBMSCs

To clarify the distinct role of STAT5A and STAT5B in osteogenesis of hBMSCs, I knocked down STAT5A or STAT5B using each siRNA and I also treated hBMSCs with a STAT5 inhibitor. siRNA mediated knockdown of STAT5A promoted osteoblast differentiation, while siRNA mediated knockdown of STAT5B had no effect **(Fig. 6a and 6b)**.

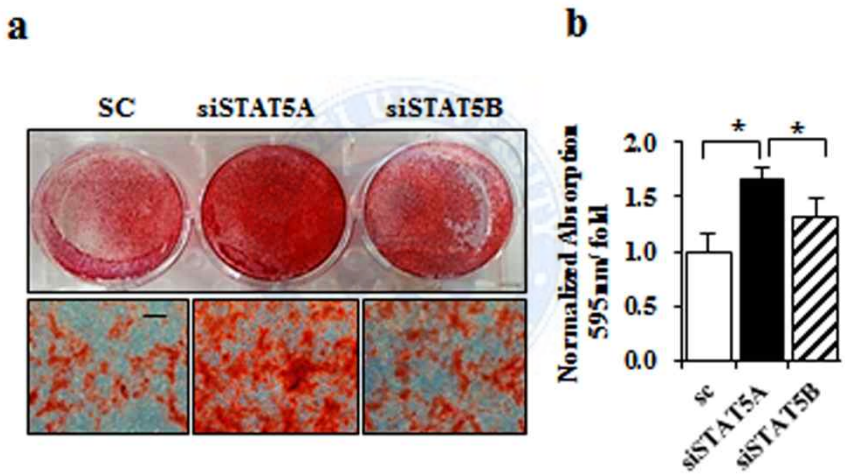

Figure 6. Induced osteoblastic differentiation through the increased DLX5 expression by siSTAT5A in hBMSCs. (a) Alizarin Red S staining suppression effect of STAT5A and STAT5B on osteogenesis using target siRNA. Staining was performed at osteogenesis 14 days. Scale bar, 30 μm. **(b)** Quantification of alizarin red S staining. I then tested whether STAT5A regulates the expression of DLX5.

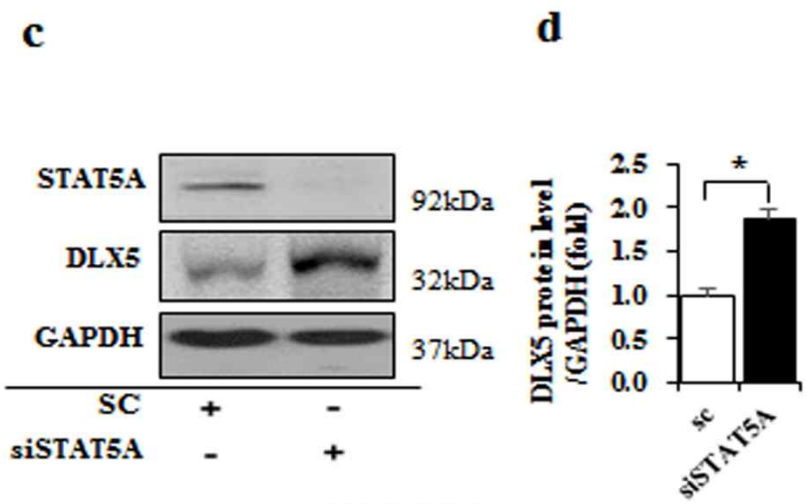

Figure 6. Induced osteoblastic differentiation through the increased DLX5 expression by siSTAT5A in hBMSCs. siRNA- mediated knockdown of STAT5A increased DLX5 protein expression. **(c)** Western blot analysis for protein expression level of DLX5 by silencing of STAT5A and STAT5B. **(d)** Quantification of DLX5 protein level was compared with GAPDH expression level.

Consistently, a STAT5 inhibitor induced a mineral accumulation in a dose-dependent manner at 14th day after the induction of osteogenesis **(Fig. 7a)**. At the dose which STAT5 inhibitor exhibited its maximal effect (10μM), STAT5 inhibitor increased a mineral accumulation about 2.5-fold over the vehicle control **(Fig. 7b)**. Accordingly, a STAT5 inhibitor increased DLX5 mRNA and protein expression in a dose-dependent manner in hBMSCs **(Fig. 7c and 7d)**.

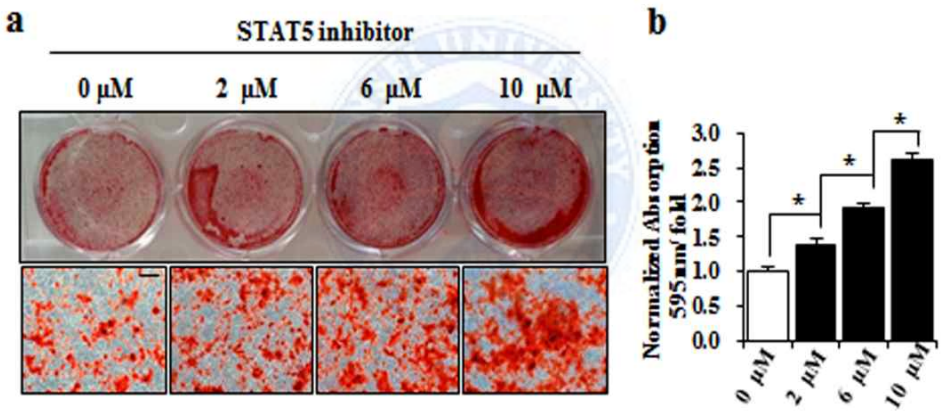

Figure 7. Induced osteoblastic differentiation through the increased DLX5 expression by STAT5 inhibitor in hBMSCs. (a) Alizarin red S staining to determine the effect of STAT5 inhibitor (sc-355979) during osteogenesis of hBMSCs. STAT5 inhibitor was used with the concentrations of 0, 2, 6, and 10μM. Staining was performed at osteogenesis 14 days. Scale bar, 30 μm. **(b)** Quantification of alizarin red S staining.

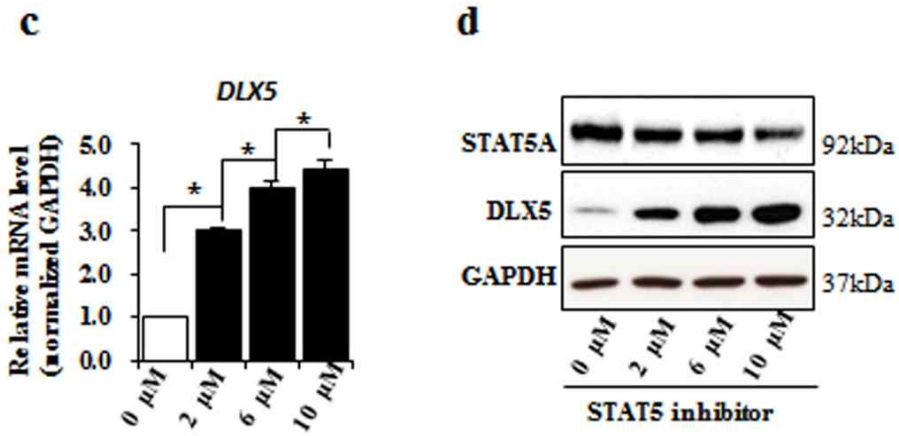

Figure 7. Induced osteoblastic differentiation through the increased DLX5 expression by STAT5 inhibitor in hBMSCs. (c) Analysis of DLX5 mRNA level by STAT5 inhibitor (10μM) treatment. **(d)** Western blot analysis for protein expression level of DLX5 by STAT5 inhibitor treatment. All experiments were performed in triplicate and determined by Student's t-test. All data are the mean ± S.D. (* $P < 0.05$, ** $P < 0.01$).

Furthermore, DLX5 promoter assays showed that STAT5 inhibitor partially reversed DLX5 activity which was decreased by STAT5A **(Fig. 7e)**.

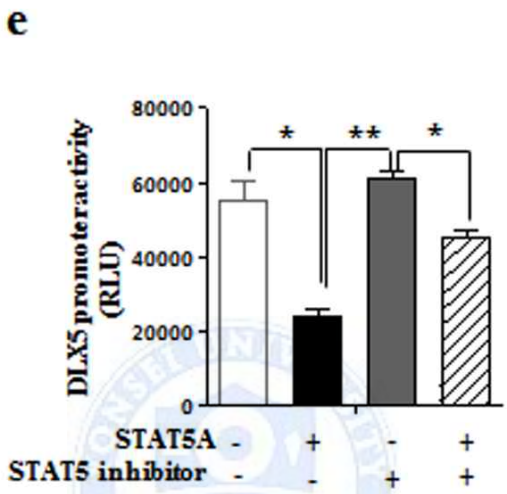

Figure 7. Relative DLX5 promoter activity by STAT5 suppression with STAT5 inhibitor. (e) STAT5 inhibitor was treated after 6hrs of transfection. Luciferase activity was normalized with *renilla*. All experiment were performed in triplicate and determined by Student's t-test. All data are the mean ± S.D. (* $P < 0.05$, ** $P < 0.01$).

3. STAT5A directly regulates DLX5 in osteoblasts

To examine the relation between STAT5A and osteogenic transcriptional regulators such as RUNX2, DLX5 and OSX, the luciferase assays for each factors were performed at 5th day after the osteogenesis of hBMSCs. STAT5A reduced DLX5 promoter activity in a dose-dependent manner **(Fig. 8a)**, while RUNX2 and OSX promoter activities were not changed **(Fig. 8b)**. To identify the detail mechanism by which STAT5A suppress DLX5 activity, I first predicted a STAT5A binding site within the DLX5 promoter region **(Fig. 1 upper, asterisk)** using the Transcription Element Search System (TESS). I then designed truncated constructs of DLX5 promoter **(Fig. 1 bottom)**. Promoter assays showed significantly decreased DLX5 activity in the constructs containing the STAT5A binding site relative to the control, whereas no change in the construct without STAT5A binding site **(Fig. 8c)**.

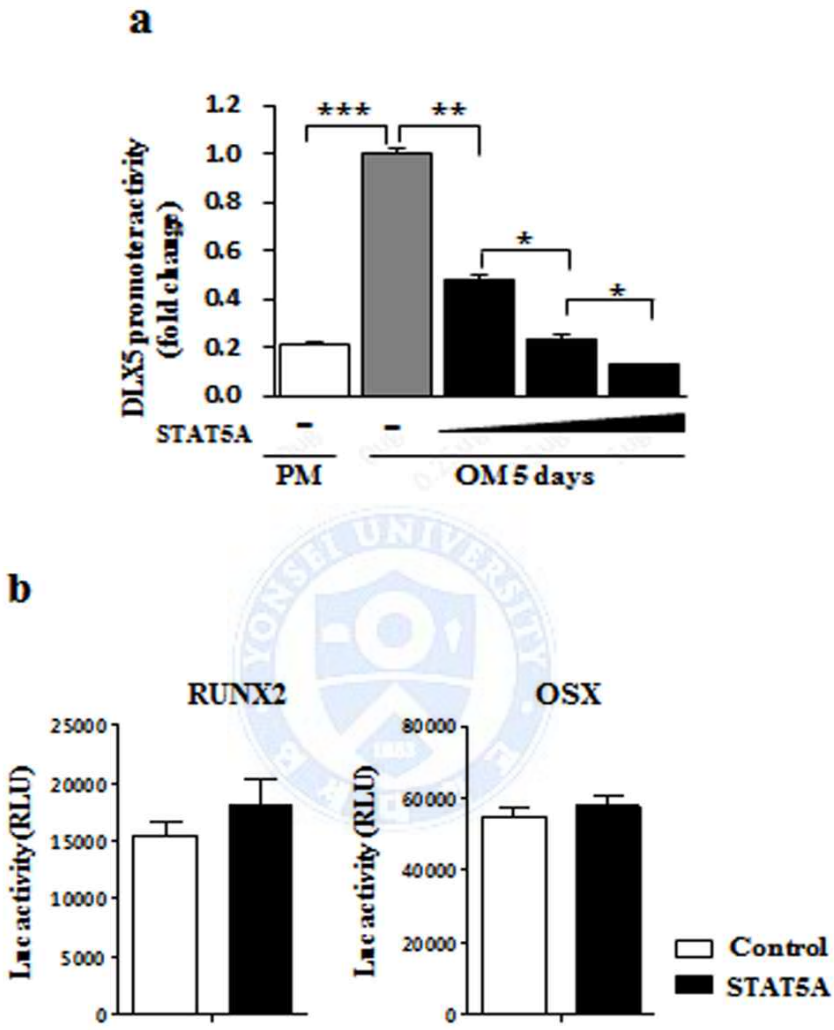
a
DLX5 promoter activity (fold change)
1.2
1.0
0.8
0.6
0.4
0.2
0.0
***
**
*
*
STAT5A
-
-
PM
OM 5 days
b
RUNX2
OSX
Luc activity (RLU)
25000
20000
15000
10000
5000
0
80000
60000
40000
20000
0
Control
STAT5A

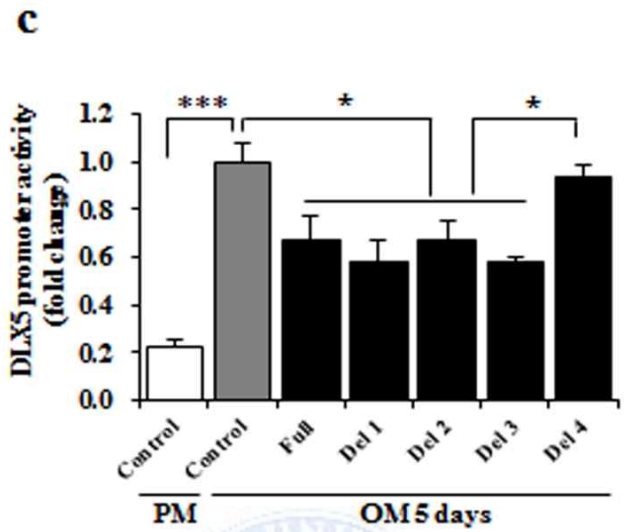

Figure 8. Decreased transcriptional activity of DLX5 by STAT5A during osteogenesis in hBMSCs. (a) Relative promoter activity of DLX5 by increasing amount of STAT5A transfected. The overexpression vector of STAT5A was used from 0μg to 1μg amount. **(b)** Promoter activity of osteoblast transcriptional factors by STAT5A. Relative promoter activity of Runx2 and Osx by STAT5A. The overexpression vector of STAT5A was used 1μg concentration. At 4th day after overexpression and 2nd day after osteogenesis, the cells were harvested and luciferase activity was normalized with renilla. **(c)** Relative transcriptional activity of truncated DLX5 promoter vectors depending on STAT5A binding prediction site. All experiment were performed in triplicate and determined by Student's t-test. All data are the mean ± S.D. (* $P < 0.05$, ** $P < 0.01$, *** $P < 0.001$).

Furthermore, ChIP assays showed that osteogenic stimulation for 5 days induced recruitment of STAT5A to the DLX5 promoter, supporting direct regulation of DLX5 by STAT5A **(Fig. 8d and 8e)**.

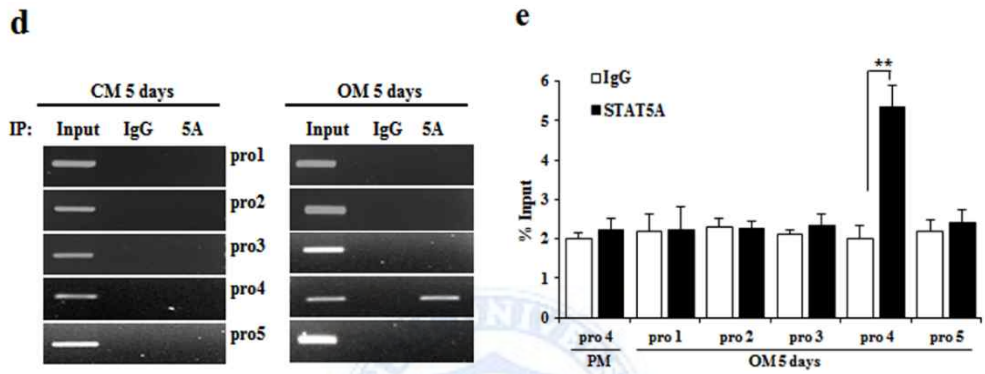

Figure 8. Localization of the element in the DLX5 promoters responsible for transcriptional repression by STAT5A. **(d)** Chromatin immune-precipitation (ChIP) assay to assess direct binding region of STAT5A to the DLX5 promoter. PCR amplification for combined DLX5 promoter region was performed with specific primers such as pro1 to pro 5 in the DLX5 promoter. **(e)** Quantification of STAT5A binding amounts to the DLX5 promoter region. All experiment were performed in triplicate and determined by Student's t-test. All data are the mean ± S.D. (** $P <$ 0.01).

4. STAT5A deletion in mice leads to high bone mass and protects against age-related osteoporosis

To determine the *in vivo* role of STAT5A in the skeletal development, I generated mice with a global deletion of *Stat5a* (referred to herein as *Stat5a*$^{-/-}$**(Fig. 9a)**. According to whole mount alizarin red/alcian blue–stained skeletal preparations, general aspects of skeletal development had no difference between E19.5 embryos of *Stat5a*$^{-/-}$ *mice* (KO) and wild type (WT) mice **(Fig. 9b)**. However, postnatal histologic analysis using Masson's trichrome staining revealed that trabecular bone mass in long bones was markedly increased in *Stat5a*$^{-/-}$ mice than in wild type mice at 10 weeks and 40 weeks **(Fig. 9c)**. Microcomputed tomography (μCT) analysis in long bone showed that *Stat5a* deletion resulted in increased trabecular and cortical bone mass relative to wild type mice in 10 weeks and 40 weeks **(Fig. 9d and 9e)**.

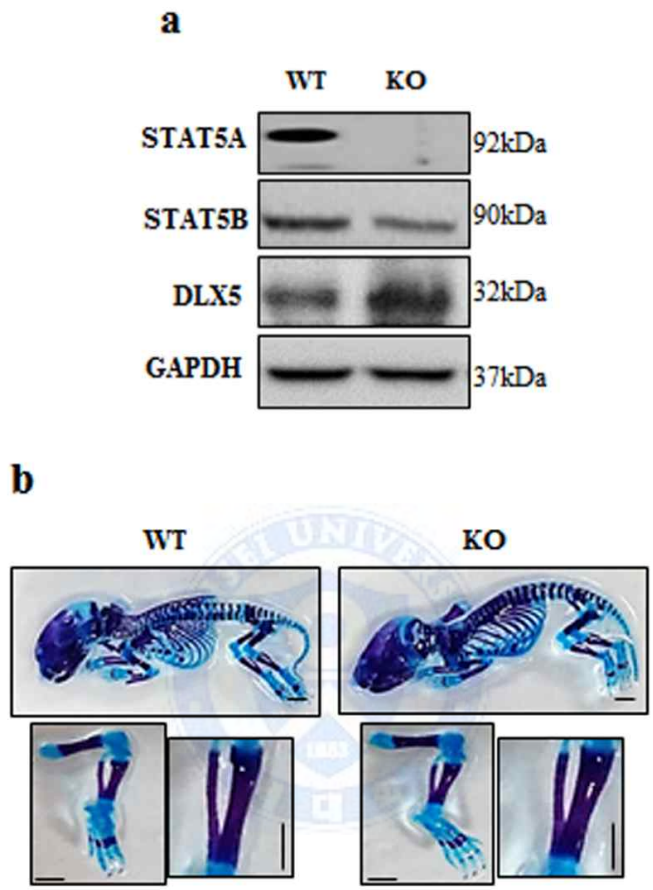

Figure 9. Increased bone formation of *stat5a*$^{-/-}$ mice. (a) Western blotting for analysis of DLX5 protein expression level at 10 weeks old male *Stat5a*$^{-/-}$ and wild type mice spleen. **(b)** Skeletal phenotype of *Stat5a*$^{-/-}$ and wild type mice. Whole-mount alizarin red S and alcian blue staining of embryos (E19.5) and hindlimb from *Stat5a*$^{-/-}$ and wild type mice. Scale bars: 2 mm (top), 1 mm (hindlimb), and 2.5 mm (tibia) (*n* = 8 per each group).

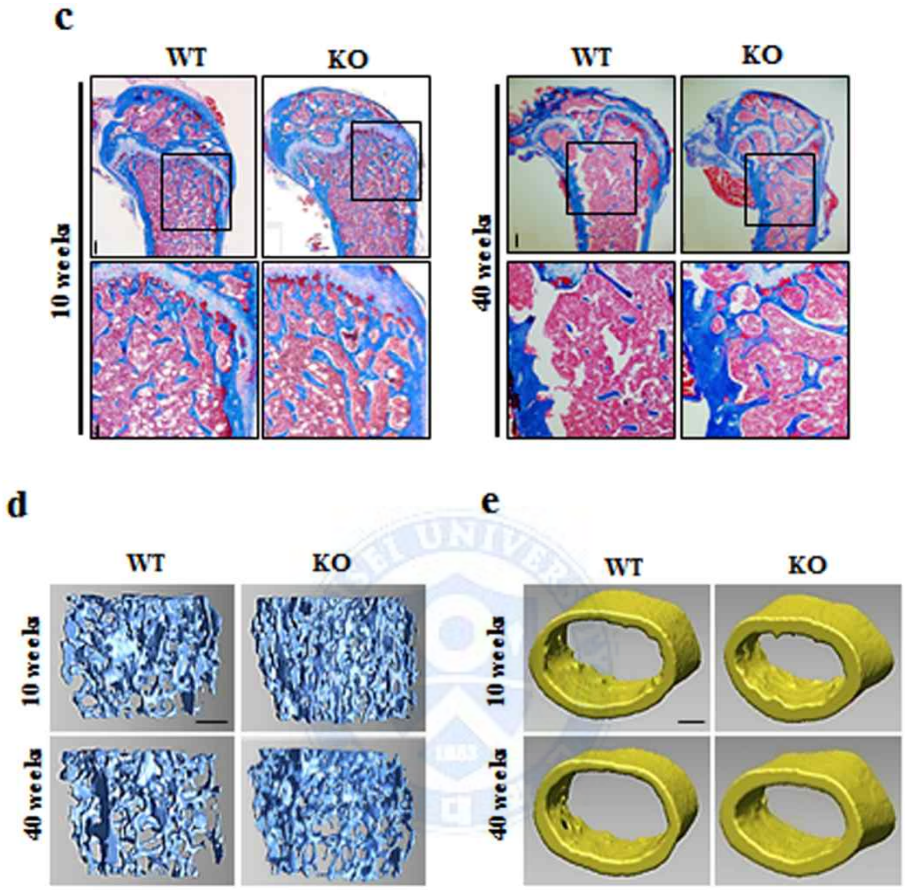

Figure 9. Increased bone formation of *stat5a*$^{-/-}$ mice. (c) Masson's trichrome staining of a longitudinal sections at 10 and 40 weeks old male *Stat5a*$^{-/-}$ and wild type femurs. Scale bar: 500 μm (top) and 200 μm (bottom) (n = 10 per each group and 8 section histology analysis). **(d)** Representative micro-CT images of trabecular bone at 10 and 40 weeks old male *Stat5a*$^{-/-}$ and wild type femurs. Scale bars, 0.5 mm (total n = 20 per 10 weeks group and 12 for 40 weeks). **(e)** Representative micro-CT images of cortical bone at 10 and 40 weeks old male *Stat5a*$^{-/-}$ and wild type femurs. Scale bars, 0.5 mm (total n = 20 per 10 weeks group and 12 for 40 weeks).

Various μCT parameters of trabecular bones increased in *Stat5a*$^{-/-}$ mice compared to wild type mice **(Fig. 9f-9j)**. Notably, I found that *Stat5a* deletion reversed the age-related reductions of bone mass and bone mineral density in 40-week old mice, suggesting that *Stat5a* deletion has a protective effect against age-related osteoporosis. Additionally, cortical thickness which is one of important factors to determine a mechanical strength was significantly higher in *Stat5a*$^{-/-}$ mice compared to wild type mice **(Fig. 9k)**. Cortical cross-sectional area (Cs. area) and cortical bone volume were also higher in *Stat5a*$^{-/-}$ mice compared to wild type mice **(Fig. 9l and 9m)**. Biomechanical properties of the femurs were assessed by three-point bending, and *Stat5a* deletion resulted in significant increase of bone strength compared to wild type mice (**Fig. 9n)**. Taken together, out results suggest a role for STAT5A in the maintenance of bone mass and strength.

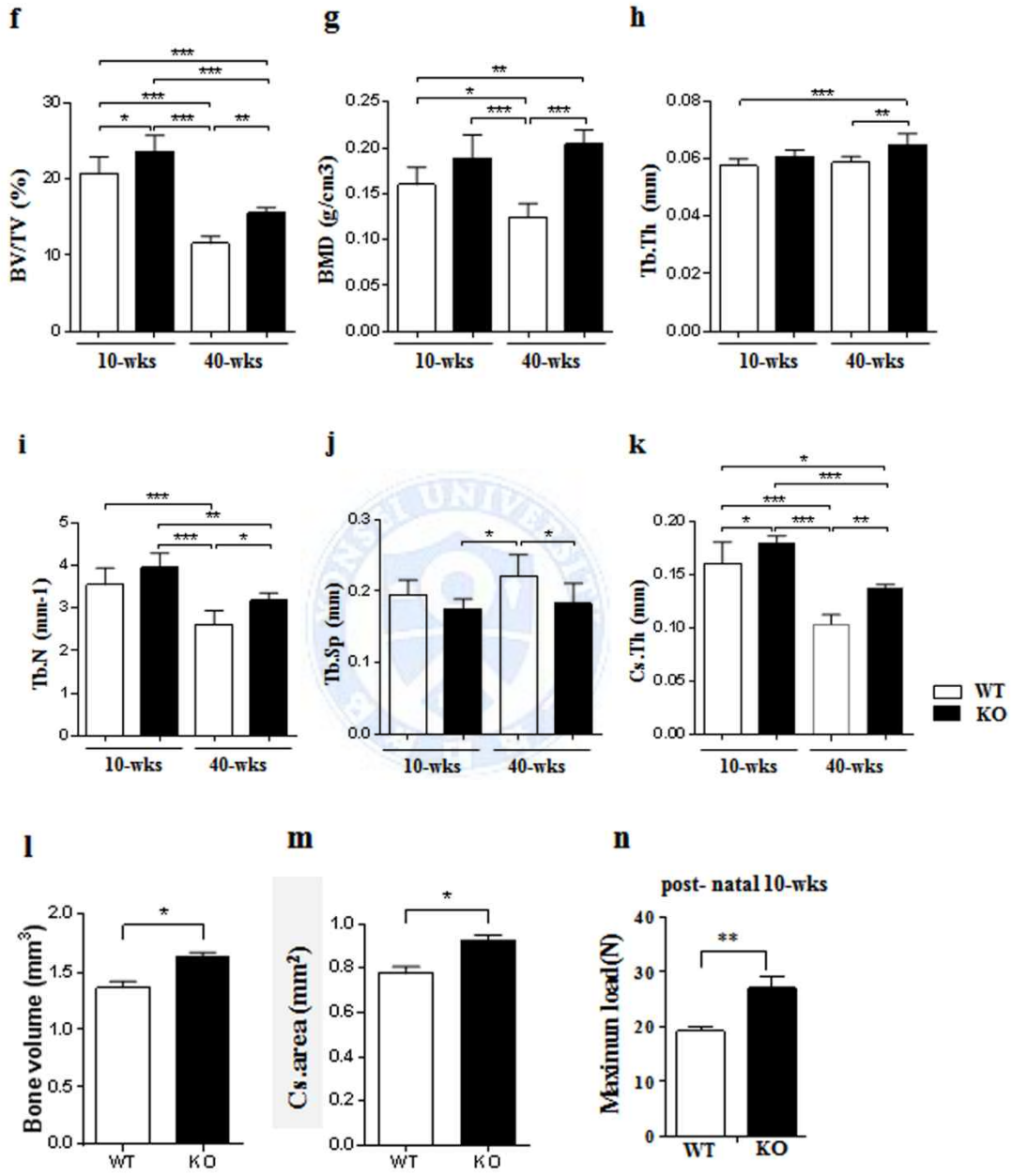
f
BV/TV (%)
10-wks
40-wks
g
BMD (g/cm3)
10-wks
40-wks
h
Tb.Th (mm)
10-wks
40-wks
i
Tb.N (mm-1)
10-wks
40-wks
j
Tb.Sp (mm)
10-wks
40-wks
k
Cs.Th (mm)
10-wks
40-wks
WT
KO
l
Bone volume (mm3)
WT
KO
m
Cs.area (mm2)
WT
KO
n
post- natal 10-wks
Maximun load(N)
WT
KO

Figure 9. Increased bone formation of *stat5a*$^{-/-}$ mice. (f-k) Quantitative micro-CT analysis of trabecular bone parameters at 10 weeks old male *Stat5a*$^{-/-}$ and wild type femurs, including (f) bone volume fraction ratio (BV/TV), (g) Volumetric BMD of trabecular bone, (h) trabecular thickness (Tb.Th), (i) trabecular number (Tb.N), (j) trabecular separation (Tb.Sp) are shown. (n = 10 for each group). **(k-m)** Quantitative micro-CT analysis of cortical bone parameters at 10 weeks old male *stat5a*$^{-/-}$ and wild type femurs, with (k) Cross-sectional thickness (Cs.Th) of cortical bone, (l) bone volume, and (m) cross-sectional area (Cs. area) are shown. (n = 10 for each group). **(n)** Maximum load on femurs from post-natal 10 weeks mice (n= 8 for each group). All parametric data were analyzed with two-tailed Student's t tests. And nonparametric data were analyzed using a Mann-Whitney test. All error bar indicate S.D. (* $P < 0.05$, ** $P < 0.01$, *** $P < 0.001$).

5. STAT5A deletion promotes osteogenic differentiation in mBMSCs

To investigate osteoblast activity of mouse bone marrow-derived stromal cells (mBMSCs), mBMSCs were isolated from *Stat5a* $^{-/-}$ mice and wild type mice. *Stat5a*$^{-/-}$ mBMSCs showed significantly higher baseline ALP activity compared to wild type mice **(Fig. 10a and 10b)**. Regardless of ages, mineral accumulations in *Stat5a*$^{-/-}$ mBMSCs were markedly higher compared to wild type mice at 8th day after the induction of osteogenesis **(Fig. 10c and 10d)**. Interestingly, a mineral accumulations in 30-week old *Stat5a*$^{-/-}$ mBMSCs was decreased compare to 10-week old *Stat5a*$^{-/-}$ mBMSCs, but comparable to 10-week old wild type mice **(Fig. 10d)**.

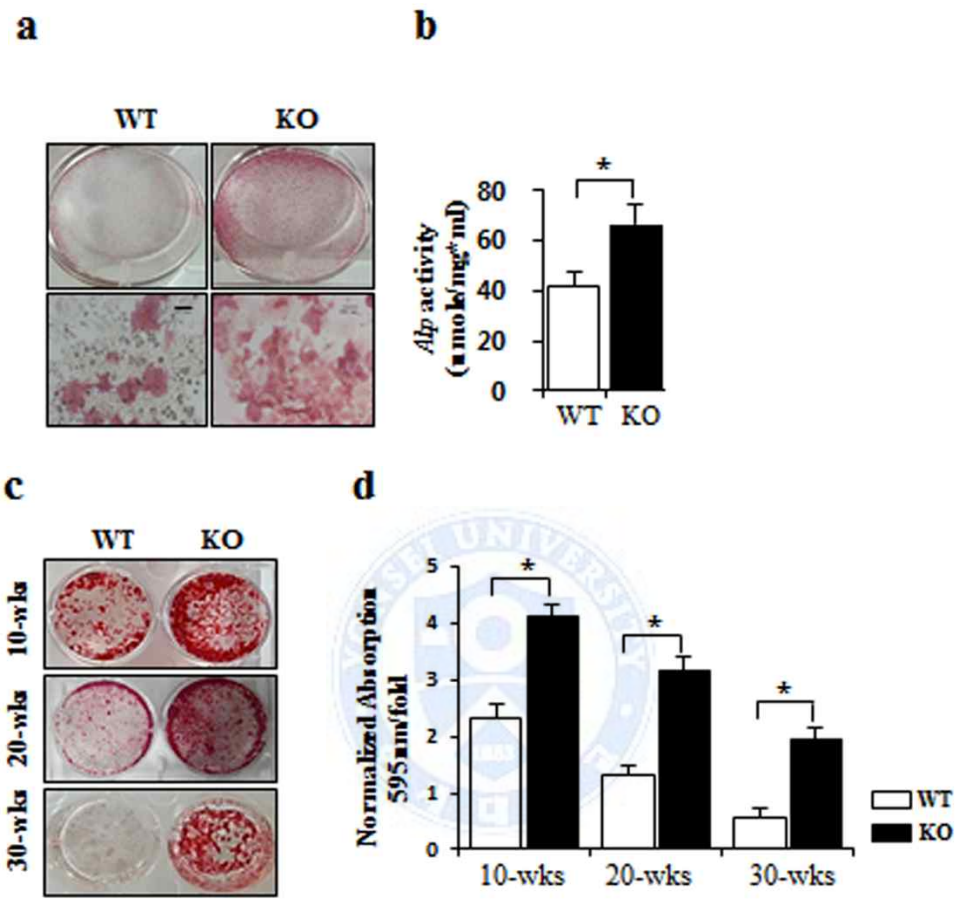

Figure 10. Induced osteoblast differentiation in *Stat5a*$^{-/-}$ mice BMSCs via up-regulation of DLX5. mBMSCs was obtained from 15 mice per each group. **(a)** ALP staining of 10 weeks old *Stat5a*$^{-/-}$ and wild type mBMSCs at osteogenesis 3rd day, as indicated. Scale bar, 60 μm. **(b)** Relative ALP activity assay at 0 day in *Stat5a*$^{-/-}$ and wild type mBMSCs. **(c)** Alizarin red S staining of 10, 20, and 30 weeks old mBMSC at 8th day after osteogenesis. **(d)** Quantification of alizarin red S staining in *Stat5a*$^{-/-}$ and wild type mBMSCs.

Accordingly, DLX5 protein and mRNA expressions in *Stat5*$^{-/-}$ mBMSCs were higher compared to wild type mice **(Fig. 10e and 10f)**. *Stat5a* deletion led to significant increases in mRNA expressions of osteogenic genes such as *Alp, Bsp, Opn*, and *Ocn* **(Fig. 10g)**.

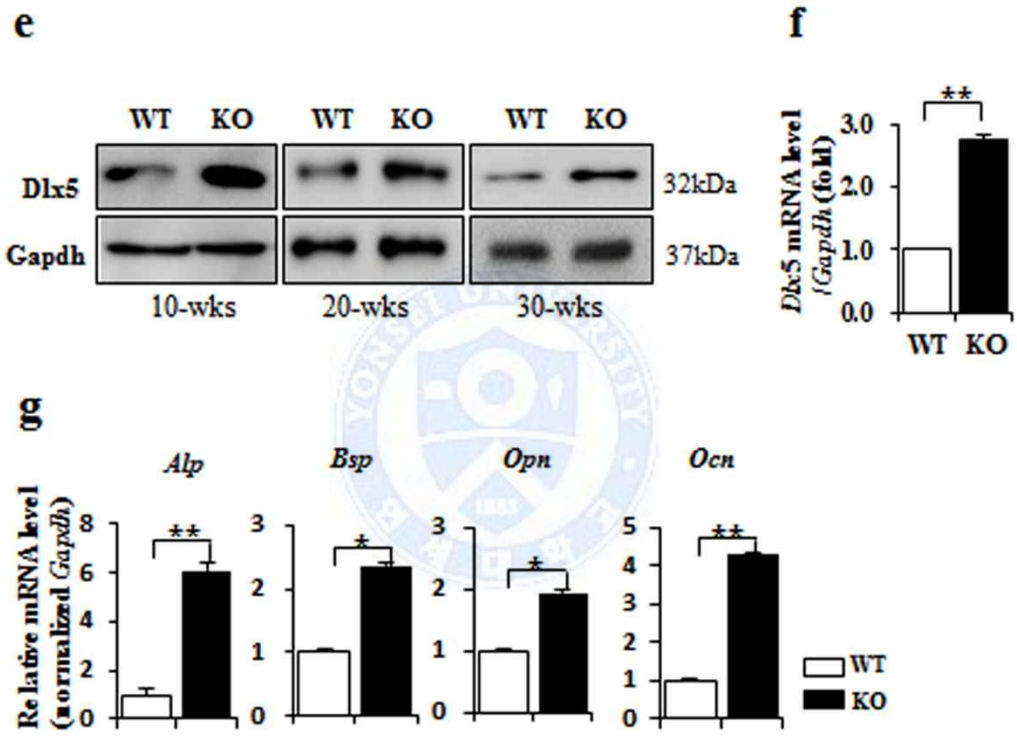

Figure 10. Induced osteoblast differentiation in *Stat5a*$^{-/-}$ mice BMSCs via up-regulation of DLX5. **(e)** Protein expression level of DLX5 in 10, 20, and 30 weeks old male *Stat5a*$^{-/-}$ and wild type mBMSCs using western blotting. **(f)** mRNA level of *Dlx5* in *Stat5a*$^{-/-}$ and wild type mBMSCs at 0 day and 3rd day after osteogenesis. **(g)** At 3rd day after osteogenic induction of mBMSCs, mRNA level of osteoblast related genes such as *Alp*, *Bsp, Opn*, and *Ocn*.

Next, I examined whether *Stat5a* overexpression reversed DLX5 expression in *Stat5a*$^{-/-}$ mBMSCs. *Stat5a* overexpression in *Stat5a*$^{-/-}$ mBMSCs significantly reversed DLX5 mRNA and protein expression which were increased by STAT5A deletion **(Fig. 10h-10j)**. In accordance with these findings, *Stat5a* overexpression decreased a mineral accumulation and calcification in *Stat5a*$^{-/-}$ mBMSCs **(Fig. 10k and 10i)**. These results demonstrate that STAT5A inhibits osteogenic differentiation by suppression of DLX5.

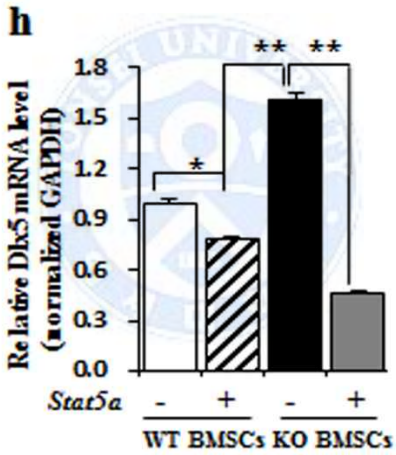

Figure 10. Induced osteoblast differentiation in *Stat5a*$^{-/-}$ mice BMSCs via up-regulation of DLX5. **(h)** Relative mRNA level of *Dlx5* depending on exogenously increased *Stat5a* expression in *Stat5a*$^{-/-}$ and wild type mBMSCs.

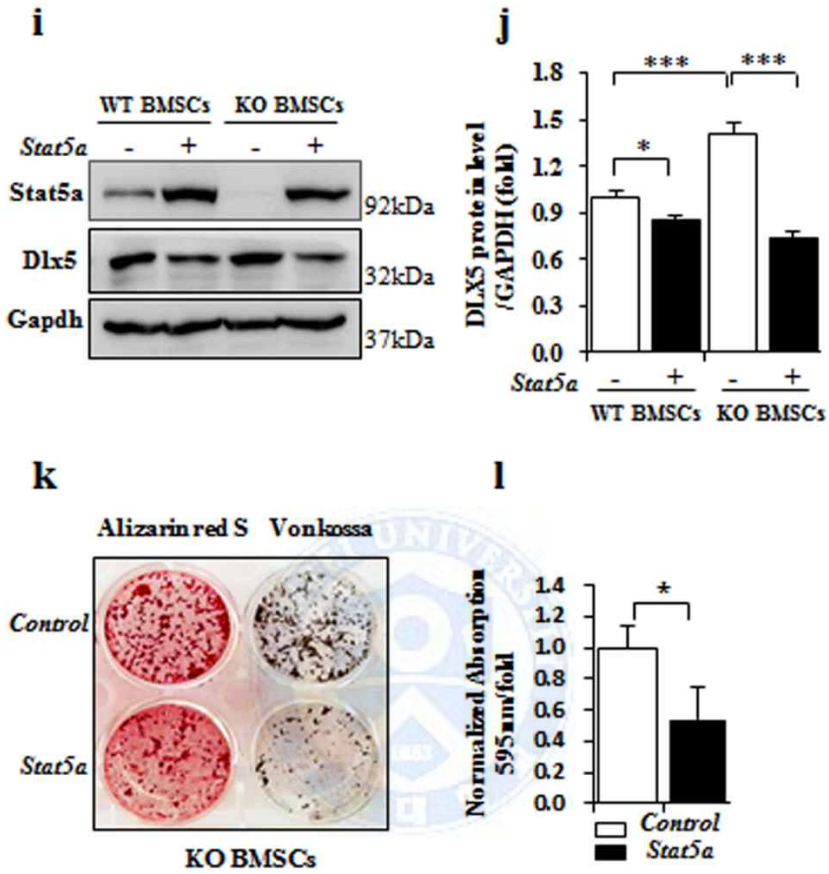

Figure 10. Induced osteoblast differentiation in *Stat5a*$^{-/-}$ mice BMSCs via up-regulation of DLX5. **(i)** DLX5 protein level when *Stat5a* was overexpressed in *Stat5a*$^{-/-}$ and wild type mBMSCs. **(j)** Quantification of DLX5 protein level when *Stat5a* was overexpressed in mBMSCs. **(k)** The osteoblast differentiation of *Stat5a*$^{-/-}$ mBMSCs by overexpression of *Stat5a* using alizarin red S and von kossa staining. **(l)** Quantification of alizarin red S staining in *Stat5a*$^{-/-}$ mBMSCs. All experiment were performed triplicate cultures of bone marrow whole cells pooled from five individual mice. All data are the mean ± S.D. ($* P < 0.05$, $** P < 0.01$, *** $P < 0.001$).

6. STAT5A deletion has no effect in osteoclast differentiation *in vitro*

Next, I examined an effect of STAT5A on osteoclast differentiation of mouse bone marrow monocytes (mBMMs). mBMMs from *Stat5a*$^{-/-}$ and wild type mice were cultured for 3~4 days in α-MEM with RANKL (receptor activator of nuclear factor-kappa B ligand) and M-CSF (macrophage colony stimulating factor). At 4th day after the induction of osteoclastogenesis, abilities of osteoclast differentiation were measured by counting of TRAP (tartrate resistant acid phosphatase) positive multinucleated osteoclasts (nuclei ≥ 3). STAT5A deletion, however, had no effect osteoclast differentiation. The numbers of TRAP positive multinucleated osteoclasts showed no difference between *Stat5a*$^{-/-}$ and wild type **(Fig. 11a and 11b)**.

Intriguingly, mRNA expression of *Rankl* and *Opg* (osteoprotegerin) were was increased in *Stat5a*$^{-/-}$ mBMSCs compared to wild type mBMSCs under the osteogenic condition **(Fig. 12a and 12b)**. Additionally, *Rankl*/*Opg* ratio, which controls the osteoclast differentiation, was also increased in *Stat5a*$^{-/-}$ mBMSCs **(Fig. 12c)**. These results indicate that STAT5A deletion had no effect in osteoclast differentiation *in vitro* but would enhance osteoclast differentiation and function *in vivo* by coupling effect between osteoblasts and osteoclasts.

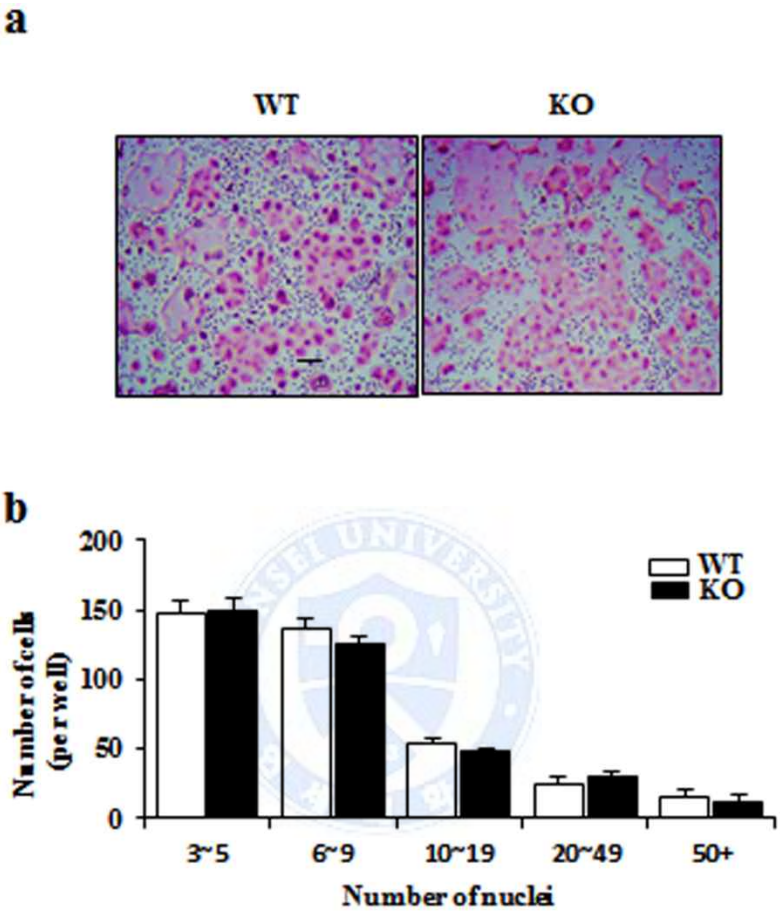

Figure 11. No difference in osteoclast differentiation *in vitro.* (a) After 4 days of osteoclastogenesis induction with M-CSF (40 ng/ml), mRANKL (20 ng/ml), RANKL-induced osteoclast formation and fusion assay of 10 weeks old male *Stat5a*$^{-/-}$ and wild type mBMMs by trap staining. Scale bar, 60 μm. (b) Quantification of TRAP-positive multinucleated cells (nuclei ≥ 3) of *Stat5a*$^{-/-}$ and wild type mBMMs.

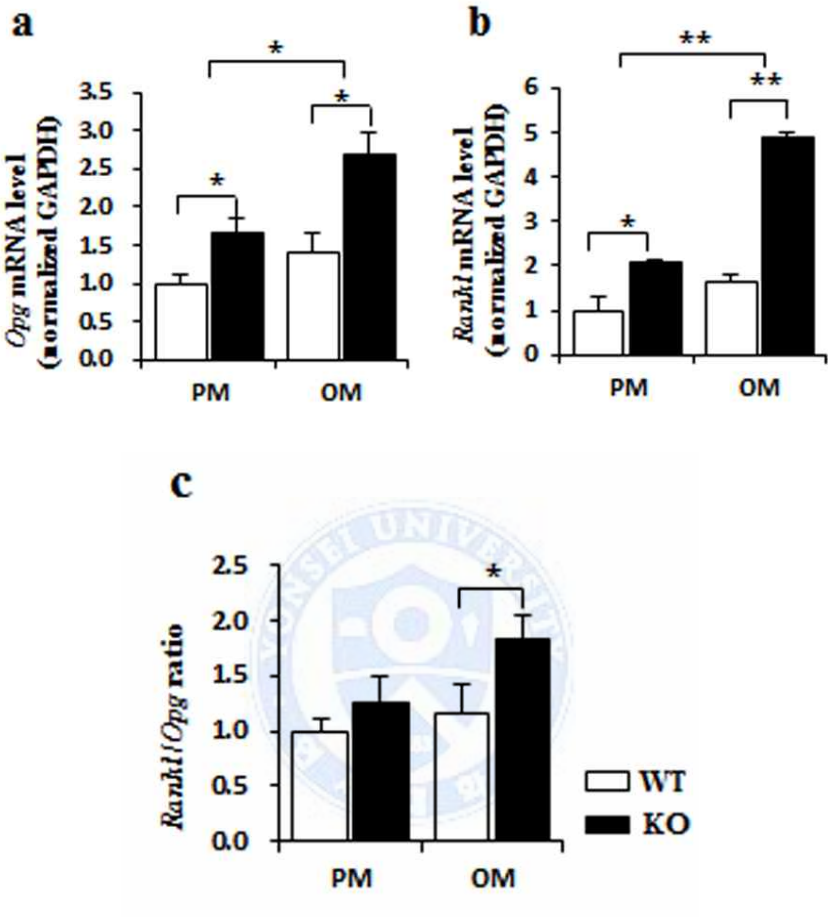

Figure 12. Increased ratio of *rankl/opg* in *stat5a*$^{-/-}$ mice BMSCs. Relative mRNA level in *Stat5a*$^{-/-}$ and wild type mBMSCs at 0 day and 5th day after osteogenesis. With **(a)** *Opg* mRNA level, **(b)** *Rankl* mRNA level, and **(c)** Ratio of *Rankl/Opg* mRNA level. All experiment were performed triplicate. All data are the mean ± S.D. (* $P < 0.05$, ** $P < 0.01$).

7. *Stat5a* deletion has negative effect in adipocyte differentiation *in vitro*

According to previous report, STAT5A increases the adipogenic differentiation of hBMSCs by correlation with pparγ[34]. To investigate this effect, BMSCs of *Stat5a*$^{-/-}$ and wild type mice were induced into adipogenic differentiation for 21days. Then lipid drops were stained with oil-red O solution. Results show that lipid drop formations were more frequent in wild type mBMSCs than *Stat5a*$^{-/-}$ mBMSCs **(Fig. 13a and 13b)**.

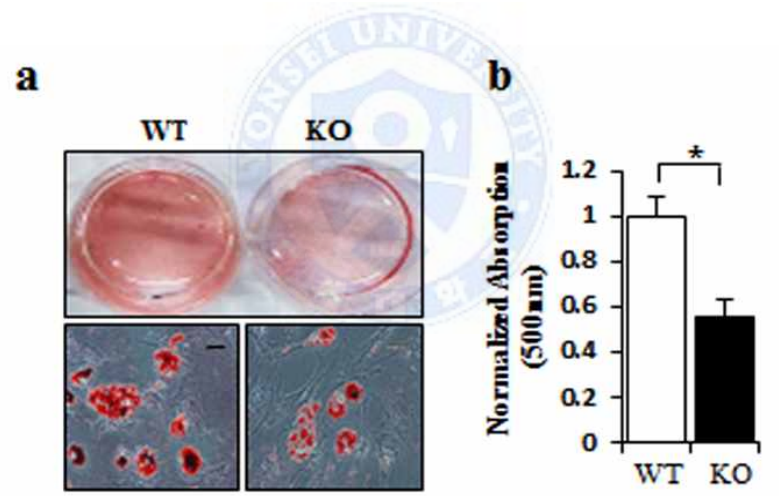

Figure 13. Reduced adipogenic differentiation in *Stat5a*$^{-/-}$ mice. (a) Oil-red O staining at adipogenesis 21 days of 10 weeks old male *Stat5a*$^{-/-}$ and wild type mBMSCs. Scale bar, Scale bar, 30 μm. **(b)** Quantification analysis of oil-red O staining.

Next, I also checked protein expressions and mRNA levels of adipocyte master regulator genes such as *pparγ* and c*/ebpα* after 5 days of adipogenesis. As expected, protein levels of both regulators were significantly decreased in *Sata5a*$^{-/-}$ BMSCs **(Fig. 13c)**. Additionally, mRNA levels of adipocyte related genes such as *adiponectin* and *leptin* were clearly reduced in *Sata5a*$^{-/-}$ BMSCs **(Fig. 13d)**. In accordance with previous differentiation data, adipocyte formation in the bone marrow of wild type femurs was more improved than in *Stat5a* $^{-/-}$ mice **(Fig. 13e)**. Taken together, STAT5A is positive regulator in adipocyte differentiation.

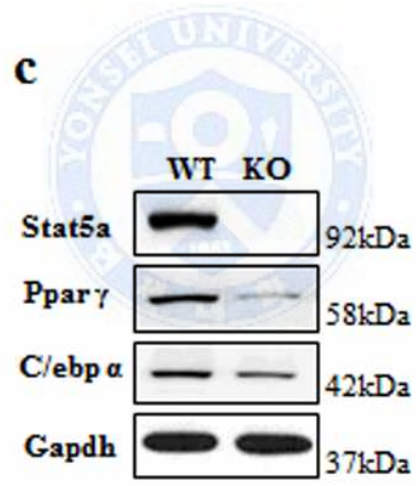

Figure 13. Reduced adipogenic differentiation in *Stat5a*$^{-/-}$ mice. (c) Western blot analysis for protein expression of adipocyte related factors in adipogenesis of *Stat5a*$^{-/-}$ and wild type mBMSC, as indicated.

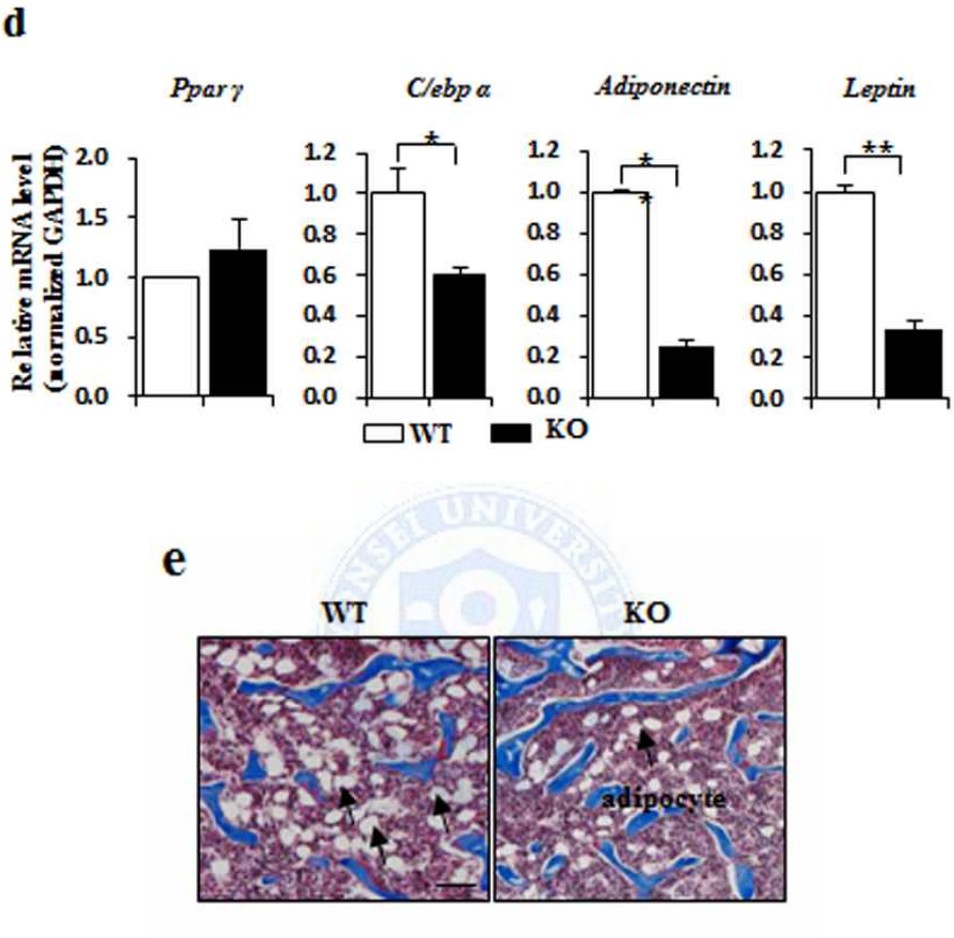

Figure 13. Reduced adipogenic differentiation in *Stat5a*$^{-/-}$ mice. (d) Relative mRNA level of adipo related genes such as *Pparγ, C/ebpα*, A*diponectin*, and *Leptin* in mBMSC by real time PCR analysis at 5th day after adipogenesis. **(e)** The adipocytes in bone marrow of *Stat5a*$^{-/-}$ and wild type mice. The distal femurs from 10 weeks old mice stained with Masson's trichrome. Scale bar, 200 μm. All experiment were performed triplicate. All data are the mean ± S.D. (* $P < 0.05$, ** $P < 0.01$).

8. STAT5A deletion promotes bone regeneration in a murine fracture model.

I next investigate the possible roles of STAT5A in a fracture healing by using a murine fracture model. I generated fracture models with femurs of 6-week old *Stat5a*$^{-/-}$ and wild type mice as previously described[28]. At post-fracture 2 and 4 weeks, I examined fracture healing using longitudinal sections of microCT images **(Fig. 14a)**. MicroCT analysis showed that bony callus at post-fracture 2 weeks increased in femurs of *Stat5a*$^{-/-}$ mice as compared to wild type mice **(Fig. 14b)**. Subsequently, bony callus at post-fracture 4 weeks decreased in femurs of *Stat5a*$^{-/-}$ mice compared to wild type mice **(Fig. 14b)**. Suggesting that STAT5A deletion accelerates fracture healing by resorption of bony callus.

To determine whether STAT5A involved the formation of cartilaginous callus along with the process of developing bony callus from cartilaginous callus, I stained femurs at post-fracture 2 and 4 weeks with Masson`s trichrome and safranin O. At post-fracture 2 weeks, area of bony callus was increased in *Stat5a*$^{-/-}$ mice compared to wild type mice **(Fig. 14c and 14d)**. But at post-fracture 4 weeks, the residual cartilaginous callus was decreased in *Stat5a*$^{-/-}$ mice compared to wild type mice **(Fig. 14e and 14f)**. These results suggest that the cartilaginous callus of the *Stat5a*$^{-/-}$ mice was more quickly transformed into the bony callus and mineralized bone compared to wild type mice.

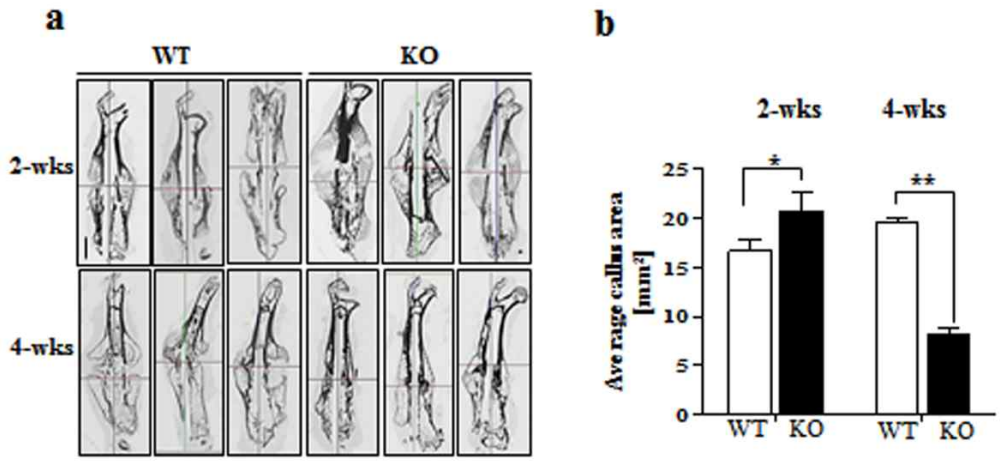

Figure 14. Enhanced bone fracture healing in *Stat5a*$^{-/-}$ mice. **(a)** Representative longitudinal sections of fractured femurs from *Stat5a*$^{-/-}$ and wild type mice at post fracture 2 weeks (2-wks) and 4 weeks (4-wks). The 6 weeks old male mice were used for fracture model. Scale bar, 4 mm (n = 16 per each group). **(b)** Quantitative analysis of newly formed callus volume at post fracture 2-wks and 4-wks.

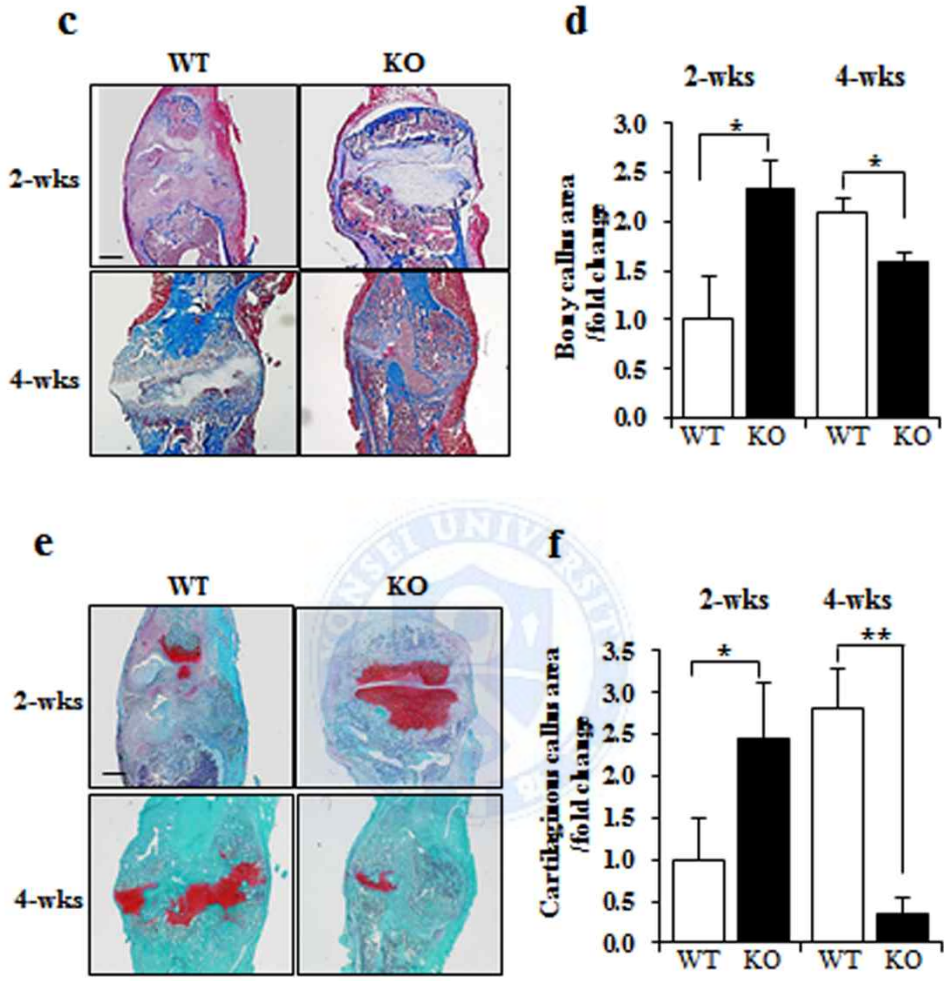

Figure 14. Enhanced bone fracture healing in *Stat5a*$^{-/-}$ mice. **(c-f)** Representative histological analysis of paraffin sections of calluses from *Stat5a*$^{-/-}$ and wild type mice at post fracture 2-wks and 4-wks stained with (c) Masson's trichrome for total collagen, (d) Quantitative analysis of bony callus area at 2-wks and 4-wks. (e) Safranin O fast green for cartilaginous callus bones, and (f) Quantitative analysis of remained cartilaginous callus area at 2-wks and 4-wks. Scale bar, 0.5 mm.

Furthermore, immunohistochemical staining showed that DLX5 expression was increased on the fracture site of *Stat5a*$^{-/-}$ mice **(Fig. 14g)**. Notably, periosteal bone of the fracture site highly expressed DLX5 in *Stat5a*$^{-/-}$ mice **(Fig. 14g, bottom)**. The numbers of osteoblasts and osteoclasts around the newly formed bone were increased in *Stat5a*$^{-/-}$ mice compared to wild type mice **(Fig. 14h)**. Similarly, biomechanical properties of regenerated femurs at post-fracture 4 weeks revealed that maximum load to failure was increased in *Stat5a*$^{-/-}$ mice compared to wild type mice **(Fig. 14i)**. Overall, these results suggest that STAT5A deletion promotes bone regeneration after a fracture.

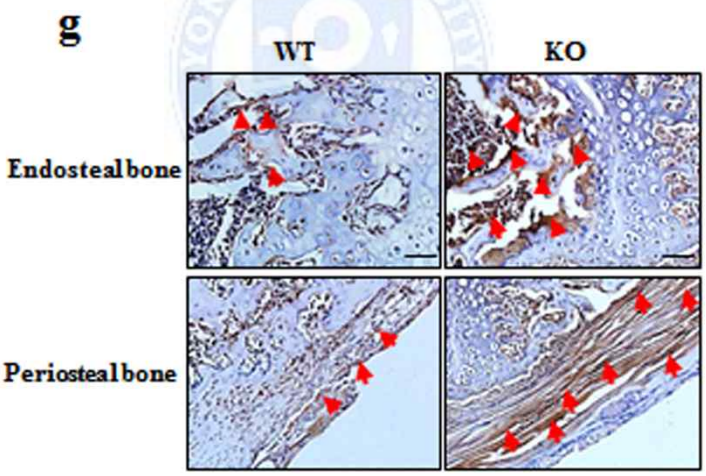

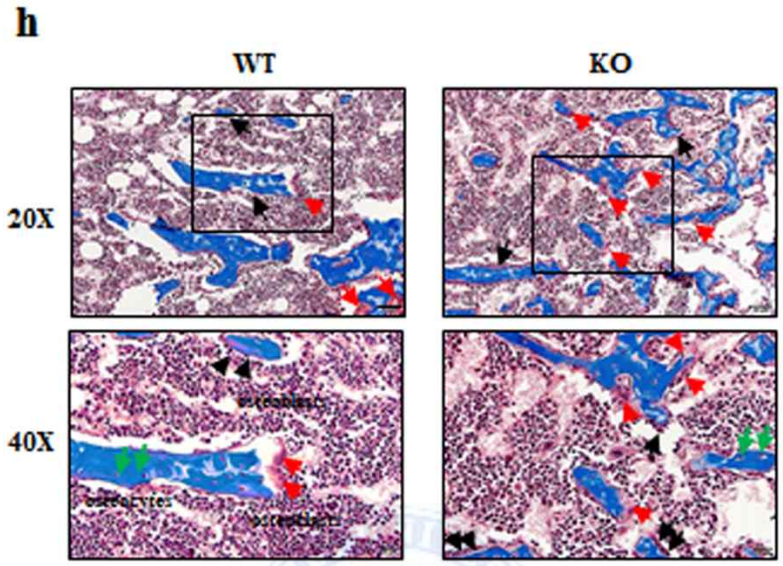
h
WT
KO
20X
40X
osteoblast
osteocyte
osteoblast

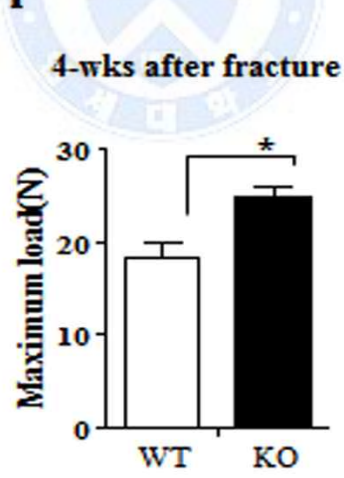
i
4-wks after fracture
Maximum load(N)
30
20
10
0
*
WT
KO

Figure 14. Enhanced bone fracture healing in *Stat5a*$^{-/-}$ mice. **(g)** Immunohistochemistry against DLX5 at post fracture 2-wks. The endosteal bone (upper) and the periosteal bone (bottom) in fractured femoral section. Scale bars; 100 μm. **(h)** Osteoblast, osteoclast, and osteocyte in regenerated bone of fractured mice femurs. Magnification; 20 x (top, scale bar; 50 μm), 40 x (bottom). Black, red, and green arrows indicated osteoblast, osteoclast, and osteocyte, respectively. **(i)** Biomechanical analysis of regenerated bone. Maximum load was assessed by three point bending method on mid-shaft femurs from post fracture 4-wks mice. All data are the mean ± S.D. (*$P < 0.05$, ** $P < 0.01$, $n = 8$ per each group)

IV. DISCUSSION

Emerging evidences suggest that Janus-activated kinase (JAK)-STAT signaling plays an important role as a negative regulator in osteoblast differentiation and bone formation[28-30]. Tajima et al. reported that inhibition of STAT1 accelerates osteoblast differentiation and bone fracture healing by regulating OSTERIX (OSX)[28], and Levy et al. reported that inhibition of STAT3 results in the augmentation of BMP-induced osteogenic differentiation[29]. Furthermore, chemical inhibitors of STAT1 and STAT3 have proposed for the treatment of skeletal bone fracture. A recent study reported that pharmacological inhibition of STAT5 reversed c-Cbl mediated osteogenesis in mBMSCs[31]. However, they had no evidence for isoform specific functions of STAT5 as a regulator of osteoblast differentiation.

Here, I found that inhibition of STAT5A by siSTAT5A significantly increased the osteoblast differentiation in hBMSCs, whereas inhibition of STAT5B by siSTAT5B had no remarkable effect in the osteogenesis (Fig. 6a and 6b). These data suggest that STAT5A may be a more important factor than STAT5B in the osteoblast differentiation of hBMSCs. Moreover, I found that *Stat5a*$^{-/-}$ mice showed higher bone mass than wild type mice. Interestingly, the increase of bone mass in *Stat5a*$^{-/-}$ mice was maintained with aging. Age-related bone loss was partially protected in *Stat5a*$^{-/-}$ mice and bone mineral densities of 40 week-old *Stat5a*$^{-/-}$ mice was comparable to those of young mice (Fig. 9c and 9d). During fracture healing process, these effects of STAT5A deletion led to enhance bone regeneration *in vivo* by stimulating bone formation. Accordingly, the mechanical strength of the regenerated bone was

significantly higher in *Stat5a*$^{-/-}$ mice compared to wild type mice (Fig. 14i), suggesting that the quality of the regenerated bone improved by STAT5A deletion. Together, these findings suggest STAT5A acts as a negative regulator of osteoblast differentiation and bone formation.

For an unbiased search for osteogenic transcriptional factors affected by STAT5A, I performed the luciferase reporter assay for well-known transcriptional factors, such as RUNX2, OSX, and DLX5. We found that STAT5A down-regulated DLX5, not RUNX2 and OSX (Fig. 8b). Additionally, I identified a STAT5A binding region on DLX5 promoter by ChIP assay (Fig. 8d and 8e). Thus, I focused on DLX5 as a target of STAT5A in osteoblast differentiation of hBMSCs. Previous studies have reported that DLX5 activity is required for RUNX2 expression under BMP signaling[32-34]. One study reported that *Dlx5* is a central regulator for bone homeostasis through direct regulation of osteogenesis[35]. I found that ALP activity and DLX5 expression in *Stat5a*$^{-/-}$ mBMSCs were higher than those in wild type mice during osteogenic differentiation (Fig. 10a and 10b). STAT5A overexpression in *Stat5a*$^{-/-}$ mBMSCs decreased DLX5 expression and impaired the osteogenic differentiation (Fig. 10k and 10l). These results indicated that DLX5 expression is controlled by STAT5A.

Intriguingly, I found that DLX5 activated STAT5 promoter activity (data not shown), while STAT5A reduced promoter activity of DLX5. Also, protein levels of STAT5A and DLX5 show conflicting manner during osteogenesis (Fig. 3b). I show that STAT5A expression increased and DLX5 expression decreased at late stage of osteogenesis. Overexpression of DLX5 does not affect early stage but prevents terminal stage of osteogenic differentiation *in vitro*[36]. However, in this study, *Stat5a*$^{-/-}$

mBMSCs had relatively higher expression of DLX5 than wild type, the mineralization of *Stat5a*$^{-/-}$ mBMSCs was better than that of wild type. Ryoo et al. reported that DLX5 expresses similar pattern with OCN during osteogenic differentiation and also temporary overexpression or repression of DLX5 has negative effects on *Ocn* expression, but DLX5 regulates only hyperactive level of *Ocn* gene expression[12]. Thus, I considered that the calcification of *Stat5a*$^{-/-}$ mMSCs was not repressed in osteogenesis, regardless of increased DLX5 expression. These results suggest that the negative feedback between STAT5A and DLX5 may present during osteoblast differentiation.

In the present study, I considered that the increase of DLX5 expression which is caused by STAT5A deletion is especially effective in periosteal bone remodeling that leads to greater mechanical strength in *Stat5a*$^{-/-}$ mice bone when compared to wild type. This speculation can be supported by this results showing that DLX5 expression is predominant in the periosteal bone (Fig. 14g), which might represent osteoblasts at a specific stage of differentiation[13,37,38]. Overall, these studies demonstrate that STAT5A deletion promotes osteoblast activity and plays an important role in callus formation and remodeling.

The balance between osteogenesis and adipogenesis is important for the maintenance of bone structure and volume[25,39-41]. In our previous studies, we demonstrated that upregulation of STAT5A by PPARγ accelerated a formation of lipid droplet during adipogenesis of hBMSCs. Conversely, inhibition of STAT5A suppressed adipogenic differentiation[25]. In this study, the opposite levels of osteoblast- and adipocyte-related genes demonstrate that the correlation between DLX5 and

STAT5A is important in balancing osteogenesis and adipogenesis.

The balance between bone formation and bone resorption is also essential for bone homeostasis. This process is known to be regulated by the OPG-RANK-RANKL pathway[42,43]. Because deletion of *Stat5a* had no effect on osteoclast differentiation, I considered the effect of osteoblast/osteoclast coupling. These results show that *Stat5a*$^{-/-}$ osteoblasts are comparatively undifferentiated to osteoclastogenesis, but that osteoclast activity could be increase via osteoblast/ osteoclast coupling effects in *Stat5a*$^{-/-}$ mice. Therefore, these findings that the deletion of STAT5A increased DLX5 expression *in vitro* and *in vivo,* suggest that DLX5 may functionally contribute to the observed induction of osteogenic functionally contribute to the observed induction of osteogenic differentiation and bone formation.

Ⅴ. CONCLUSION

I figured out that STAT5A attenuates osteoblast differentiation by regulating DLX5 *in vitro* and STAT5A deletion promotes bone formation, prevents age-related osteoporosis and accelerates fracture healing *in vivo*. These results suggest that targeting STAT5A inhibition as a new therapeutic strategy to control bone homeostasis and fracture healing.

REFERENCES

1. Beyer Nardi N, da Silva Meirelles L. Mesenchymal stem cells: isolation, in vitro expansion and characterization. Handb Exp Pharmacol 2006:249-82.
2. Delorme B, Charbord P. Culture and characterization of human bone marrow mesenchymal stem cells. Methods Mol Med 2007;140:67-81.
3. Javazon EH, Beggs KJ, Flake AW. Mesenchymal stem cells: paradoxes of passaging. Exp Hematol 2004;32:414-25.
4. Martin DR, Cox NR, Hathcock TL, Niemeyer GP, Baker HJ. Isolation and characterization of multipotential mesenchymal stem cells from feline bone marrow. Exp Hematol 2002;30:879-86.
5. Pittenger MF, Mackay AM, Beck SC, Jaiswal RK, Douglas R, Mosca JD, et al. Multilineage potential of adult human mesenchymal stem cells. Science 1999;284:143-7.
6. Dragojevic J, Logar DB, Komadina R, Marc J. Osteoblastogenesis and adipogenesis are higher in osteoarthritic than in osteoporotic bone tissue. Arch Med Res 2011;42:392-7.
7. Aubin JE. Regulation of osteoblast formation and function. Rev Endocr Metab Disord 2001;2:81-94.
8. Lian JB, Javed A, Zaidi SK, Lengner C, Montecino M, van Wijnen AJ, et al. Regulatory controls for osteoblast growth and differentiation: role of Runx/Cbfa/AML factors. Crit Rev Eukaryot Gene Expr 2004;14:1-41.
9. Franceschi RT, Xiao G. Regulation of the osteoblast-specific transcription factor, Runx2: responsiveness to multiple signal transduction pathways. J Cell Biochem 2003;88:446-54.
10. Karsenty G. Transcriptional control of skeletogenesis. Annu Rev Genomics Hum Genet 2008;9:183-96.

11. Holleville N, Mateos S, Bontoux M, Bollerot K, Monsoro-Burq AH. Dlx5 drives Runx2 expression and osteogenic differentiation in developing cranial suture mesenchyme. Dev Biol 2007;304:860-74.
12. Ryoo HM, Hoffmann HM, Beumer T, Frenkel B, Towler DA, Stein GS, et al. Stage-specific expression of Dlx-5 during osteoblast differentiation: involvement in regulation of osteocalcin gene expression. Mol Endocrinol 1997;11:1681-94.
13. Acampora D, Merlo GR, Paleari L, Zerega B, Postiglione MP, Mantero S, et al. Craniofacial, vestibular and bone defects in mice lacking the Distal-less-related gene Dlx5. Development 1999;126:3795-809.
14. Agaisse H, Petersen UM, Boutros M, Mathey-Prevot B, Perrimon N. Signaling role of hemocytes in Drosophila JAK/STAT-dependent response to septic injury. Dev Cell 2003;5:441-50.
15. Ivashkiv LB, Hu X. Signaling by STATs. Arthritis Res Ther 2004;6:159-68.
16. Cumaraswamy AA, Gunning PT. Progress towards direct inhibitors of Stat5 protein. Horm Mol Biol Clin Investig 2012;10:281-6.
17. Liao Z, Gu L, Vergalli J, Mariani SA, De Dominici M, Lokareddy RK, et al. Structure-Based Screen Identifies a Potent Small Molecule Inhibitor of Stat5a/b with Therapeutic Potential for Prostate Cancer and Chronic Myeloid Leukemia. Mol Cancer Ther 2015;14:1777-93.
18. Grimley PM, Dong F, Rui H. Stat5a and Stat5b: fraternal twins of signal transduction and transcriptional activation. Cytokine Growth Factor Rev 1999;10:131-57.
19. Gouilleux F, Wakao H, Mundt M, Groner B. Prolactin induces phosphorylation of Tyr694 of Stat5 (MGF), a prerequisite for DNA binding and induction of transcription. Embo j 1994;13:4361-9.

20. Meyer T, Vinkemeier U. Nucleocytoplasmic shuttling of STAT transcription factors. Eur J Biochem 2004;271:4606-12.
21. Zeng R, Aoki Y, Yoshida M, Arai K, Watanabe S. Stat5B shuttles between cytoplasm and nucleus in a cytokine-dependent and -independent manner. J Immunol 2002;168:4567-75.
22. Akira S. Functional roles of STAT family proteins: lessons from knockout mice. Stem Cells 1999;17:138-46.
23. Lin JX, Leonard WJ. The role of Stat5a and Stat5b in signaling by IL-2 family cytokines. Oncogene 2000;19:2566-76.
24. Hirose J, Masuda H, Tokuyama N, Omata Y, Matsumoto T, Yasui T, et al. Bone resorption is regulated by cell-autonomous negative feedback loop of Stat5-Dusp axis in the osteoclast. J Exp Med 2014;211:153-63.
25. Jung HS, Lee YJ, Kim YH, Paik S, Kim JW, Lee JW. Peroxisome proliferator-activated receptor gamma/signal transducers and activators of transcription 5A pathway plays a key factor in adipogenesis of human bone marrow-derived stromal cells and 3T3-L1 preadipocytes. Stem Cells Dev 2012;21:465-75.
26. Naot D, Bava U, Matthews B, Callon KE, Gamble GD, Black M, et al. Differential gene expression in cultured osteoblasts and bone marrow stromal cells from patients with Paget's disease of bone. J Bone Miner Res 2007;22:298-309.
27. Park KH, Park B, Yoon DS, Kwon SH, Shin DM, Lee JW, et al. Zinc inhibits osteoclast differentiation by suppression of Ca2+-Calcineurin-NFATc1 signaling pathway. Cell Commun Signal 2013;11:74.
28. Tajima K, Takaishi H, Takito J, Tohmonda T, Yoda M, Ota N, et al. Inhibition of STAT1 accelerates bone fracture healing. J Orthop Res 2010;28:937-41.

29. Levy O, Ruvinov E, Reem T, Granot Y, Cohen S. Highly efficient osteogenic differentiation of human mesenchymal stem cells by eradication of STAT3 signaling. Int J Biochem Cell Biol 2010;42:1823-30.
30. Levy O, Dvir T, Tsur-Gang O, Granot Y, Cohen S. Signal transducer and activator of transcription 3-A key molecular switch for human mesenchymal stem cell proliferation. Int J Biochem Cell Biol 2008;40:2606-18.
31. Dieudonne FX, Severe N, Biosse-Duplan M, Weng JJ, Su Y, Marie PJ. Promotion of osteoblast differentiation in mesenchymal cells through Cbl-mediated control of STAT5 activity. Stem Cells 2013;31:1340-9.
32. Merlo GR, Zerega B, Paleari L, Trombino S, Mantero S, Levi G. Multiple functions of Dlx genes. Int J Dev Biol 2000;44:619-26.
33. Hassan MQ, Javed A, Morasso MI, Karlin J, Montecino M, van Wijnen AJ, et al. Dlx3 transcriptional regulation of osteoblast differentiation: temporal recruitment of Msx2, Dlx3, and Dlx5 homeodomain proteins to chromatin of the osteocalcin gene. Mol Cell Biol 2004;24:9248-61.
34. Ryoo HM, Lee MH, Kim YJ. Critical molecular switches involved in BMP-2-induced osteogenic differentiation of mesenchymal cells. Gene 2006;366:51-7.
35. Samee N, Geoffroy V, Marty C, Schiltz C, Vieux-Rochas M, Levi G, et al. Dlx5, a positive regulator of osteoblastogenesis, is essential for osteoblast-osteoclast coupling. Am J Pathol 2008;173:773-80.
36. Muraglia A, Perera M, Verardo S, Liu Y, Cancedda R, Quarto R, et al. DLX5 overexpression impairs osteogenic differentiation of human bone marrow stromal cells. Eur J Cell Biol 2008;87:751-61.
37. Zhang J, Zhu J, Valverde P, Li L, Pageau S, Tu Q, et al. Phenotypic analysis of Dlx5 overexpression in post-natal bone. J Dent Res 2008;87:45-50.

38. Samee N, Geoffroy V, Marty C, Schiltz C, Vieux-Rochas M, Clement-Lacroix P, et al. Increased bone resorption and osteopenia in Dlx5 heterozygous mice. J Cell Biochem 2009;107:865-72.
39. Duque G. Bone and fat connection in aging bone. Curr Opin Rheumatol 2008;20:429-34.
40. Kawai M, Devlin MJ, Rosen CJ. Fat targets for skeletal health. Nat Rev Rheumatol 2009;5:365-72.
41. Pei L, Tontonoz P. Fat's loss is bone's gain. J Clin Invest 2004;113:805-6.
42. Theoleyre S, Wittrant Y, Tat SK, Fortun Y, Redini F, Heymann D. The molecular triad OPG/RANK/RANKL: involvement in the orchestration of pathophysiological bone remodeling. Cytokine Growth Factor Rev 2004;15:457-75.
43. Atkins GJ, Kostakis P, Pan B, Farrugia A, Gronthos S, Evdokiou A, et al. RANKL expression is related to the differentiation state of human osteoblasts. J Bone Miner Res 2003;18:1088-98.

ABSTRACT (IN KOREAN)

골아세포 분화 및 골 형성에서 STAT5A 의 역할

<지도교수 이 진 우>

연세대학교 대학원 의과학과

이 경 미

사람의 골수 유래 중간엽 줄기세포 (hBMSCs)의 골분화 과정의 조절은 골형성에 중요한 영향을 준다. 골분화 과정의 분자적 메커니즘에 대한 연구가 활발함에도 불구하고, 골절치유에 작용하는 핵심인자에 대한 규명은 미흡한 실정이다. 신호전달 조절 인자인 STAT5 (Signal transducer and acivator of transcription 5)는 다양한 세포에서 cytokine 에 의해 조절되는 과정 즉, 세포의 생존, 증식, 그리고 분화에 필수적인 요소이다.

본 연구에서는 hBMSCs 의 골 분화과정에서 STAT5 의 역할을 밝히고자 하였다. STAT5 억제제와 siRNA 를 이용한 STAT5A 의 저해는 hBMSCs 의 골분화를 현저히 증가시킨 반면, STAT5B 의

저해는 대조군과 유사한 골분화능을 보여주었다. 특히, STAT5A 의 저해는 골 분화 전사인자인 DLX5 의 mRNA 및 단백질 발현을 증가시켰다. 또한, ChIP (Chromatin immunoprecipitation) 분석을 통하여 STAT5A 가 골분화 기간 동안 DLX5 의 프로모터 부위에 결합하여 전사활성을 감소시킴을 확인하였다. 더불어, STAT5A 유전자가 결핍된 마우스를 이용하여 STAT5A 가 골형성에 미치는 영향을 분석한 결과, *Stat5a* 결손 마우스에서 골형성이 대조군에 비해 현저히 증가되었음을 확인하였다. 특히, *Stat5a* 결손 마우스 BMSCs 의 골분화력 역시 활성화 되었으며, DLX5 의 단백질 발현양 또한 증가하였다. 이러한 증가된 조골세포의 활성을 검증하기 위해 *Stat5a* 결손 골절 모델을 이용하여 골절 치유력을 살펴보았다. 골절 유발 2 주 후, *Stat5a* 결손 마우스의 골절부위 신생골 형성이 대조군에 비해 증가하였고, 4 주 후 남아있는 연골성 신생골의 양은 *Stat5a* 결손 마우스에서 현저히 줄어들었음을 확인 하였다. 이는 *Stat5a* 결손 마우스의 골 리모델링 능력이 대조군에 비해 우수함을 나타낸다. 요약하면, STAT5A 의 억제는 DLX5 의 발현을 증가시킴으로써, 생체 외 골분화력 뿐만아니라, 생체 내 골형성 능력을 증가시켰다. 또한, *Stat5a* 결손 마우스의 경우, 노화로 인해

유도되는 골밀도와 골강도의 감소가 대조군에 비해 완화되어 있었다. 특히, 골절치유 모델에서 *Stat5a* 의 결손은 신생골의 형성능을 현저히 증가시켰다.

종합해보면, STA5A 는 골분화 과정 동안 DLX5 발현조절을 통해 골분화, 골형성 및 골절치유를 조절하는 중요한 전사조절 인자임을 시사한다. 따라서, STA5A 가 노화로 인해 야기되는 골다공증 및 골절과 같은 골 리모델링 관련 골격 질환의 치료 표적이 될 수 있을 것이다.

핵심되는 말: 골분화, 골형성, STAT5A, DLX5, 골리모델링

PUBLICATION LIST

Yoon DS*, **Lee KM*,** Kim SH, Kim SH, Jung YM, Kim SH, Park KH, Choi YR, Ryu HA, Choi WJ, Lee JW. Synergistic Action of Interleukin-8 and Bone Marrow Concentrate on Cartilage Regeneration through Up-Regulation of Chondrogenic Transcription Factors. Tissue Eng Part A 2015; Published.

Park KW, Choi WJ, **Lee KM,** Yoon DS, Kim SH, Lee JW. In Vivo Cartilage Formation Using Human Bone Marrow-Derived Mesenchymal Stem Cells Mixed with Fibrin Glue. J Korean Orthop Res Soc 2015; 18:43-50.

Yoon DS, Kim YH, Lee S, **Lee KM**, Park KH, Jang Y, Lee JW. Interleukin-6 induces the lineage commitment of bone marrow-derived mesenchymal multipotent cells through down-regulation of Sox2 by osteogenic transcription factors. FASEB J 2014; 28: 3273-86.

Lee S, Yoon DS, Paik S, **Lee KM**, Jang Y, Lee JW. microRNA- 495 inhibits chondrogenic differentiation in human mesenchymal stem cells by targeting Sox9. Stem Cells Dev 2014; 23:1798-808.

Hwang JS, **Lee KM**, Jung HS, Lee JW, Choi YR. Differential Expression of STATs and Its Function in Osteogenesis of Mesenchymal Stem Cells. J Korean Orthop Res Soc 2013; 16: 1-9.